patients (13). Thus, drug sensitivity appears to be one of the major determinants of the prognosis of advanced HCC patients treated with chemotherapy. Therefore, a hallmark of successful treatment would be the identification of useful biomarkers for determining the survival benefits offered by each treatment strategy.

In this study, we investigated the gene expression profiles of HCCs using serial analysis of gene expression (SAGE) to identify novel molecular markers or targets for the treatment of HCC (14–18). Here, we identified the upregulation of the *DUT* gene that encodes dUTP pyrophosphatase (dUTPase) in HCC. Markedly, HCC with a high nuclear dUTPase expression correlated with a poorly differentiated morphology and a poor prognosis. *DUT* gene knockdown not only suppressed cell proliferation but also sensitized HuH7 cells to low-dose 5-FU.

Materials and methods

Samples

All HCC tissues, adjacent non-cancerous liver tissues and normal liver tissues were obtained from 110 patients undergoing a hepatectomy between 1997 and 2006 in Kanazawa University Hospital, Kanazawa, Japan. Five normal liver tissue samples were obtained from patients undergoing surgical resection of the liver for the treatment of metastatic colon cancer. These samples were snap-frozen in liquid nitrogen immediately after resection. One hundred and five HCC and surrounding non-cancerous liver samples were obtained from patients undergoing surgical resection of the liver for HCC treatment, and part of these samples were used for the recent study (19). Three HCC and adjacent non-cancerous liver tissue samples were snap-frozen in liquid nitrogen and later used for SAGE. Twenty HCC tissues and their corresponding non-cancerous liver tissues were also snap-frozen and later used for real-time reverse transcription-polymerase chain reaction (RT-PCR) analysis, as described previously (19). Eighty-two additional HCC samples were formalin-fixed, paraffin-embedded and used for immunohistochemistry (IHC). HCC and adjacent non-cancerous liver tissues were histologically characterized, as reported elsewhere (19).

All strategies used for gene expression analysis as well as tissue acquisition processes were approved by the Ethics Committee and the Institutional Review Board of Kanazawa University Hospital. All procedures and risks were explained verbally to each patient, who then provided written informed consent.

Serial analysis of gene expression

Total RNA was purified from each homogenized tissue sample using a ToTally RNA extraction kit (Ambion Inc., Austin, TX, USA), and polyadenylated RNA was isolated using a MicroPoly (A) Pure kit (Ambion). A total of 2.5 μg of mRNA per sample was analysed by SAGE (20, 21). SAGE libraries were randomly sequenced at the Genomic Research Center (Shimadzu-Biotechnology, Kyoto, Japan), and the sequence files were analysed with SAGE 2000 software. The size of each SAGE library was normalized to 300 000 transcripts per library, and the abundance of transcripts was compared with SAGE 2000 software. Monte Carlo simulation was used for selecting genes whose expression levels were significantly different between the two libraries (22). Each SAGE tag was annotated using a gene-mapping website SAGE Genie database (http://cgap.nci.nih.gov/SAGE/) and the Source database (http://smd.stanford.edu/cgi-bin/source/sourceSearch), as described previously (23).

Quantitative reverse transcription-polymerase chain reaction

A 1 μg aliquot of each total RNA was reverse-transcribed using SuperScript II reverse-transcriptase (Invitrogen, Carlsbad, CA, USA). Real-time RT-PCR analysis was performed using the ABI PRISM 7700 sequence detection system (Applied Biosystems, Foster City, CA, USA). Using the standard curve method, quantitative PCR was performed in duplicate for each sample–primer set. Each sample was normalized relative to β actin. The assay IDs used were Hs00798995_s1 for dUTPase and Hs99999903_m1 for β actin.

RNA interference targeting *DUT*

Small interfering RNAs (siRNAs) targeting *DUT* or control (scrambled sequence) were synthesized by Dharmacon (Dharmacon Research Inc., Lafayette, CO, USA). The target sequences of *DUT* are 5′-AAGUUGU GAAAACGGACAUUC-3′ (DUT1) and 5′-CGGACAUU CAGAUAGCGCUTT-3′ (DUT2). Lipofectamine 2000™ reagent (Invitrogen) was used for transfection according to the manufacturer's instructions.

Cell proliferation assay, soft agar assay and matrigel invasion assay

Cell proliferation assays were performed using a Cell Titer96 Aqueous kit in quintuplicate (Promega, Madison, WI, USA). For the soft agar assay, 1×10^4 cells were suspended in 2 ml of 0.36% agar with growth medium and added in each well of a six-well plate containing a base layer of 0.72% agar. The plates were incubated at 37 °C in a 5% CO_2 incubator for 2 weeks. Matrigel invasion assays were performed using BD BioCoat™ Matrigel Matrix Cell Culture Inserts and Control Inserts (BD Biosciences, San Jose, CA, USA), as described in the manufacturer's instruction. 5-FU was obtained from Kyowa Kirin (Kyowa Kirin, Tokyo, Japan). All experiments were repeated at least twice.

Immunohistochemistry

Mouse monoclonal anti-dUTPase antibody M01 (Abnova Corporation, Taipei, Taiwan) and mouse antiproliferating cell nuclear antigen (PCNA) monoclonal antibody PC10 (Calbiochem, San Diego, CA, USA) were used to evaluate the immunoreactivity of HCC and adjacent non-cancerous liver samples using a Dako EnVision+^{TM} kit (Dako, Carpinteria, CA, USA), according to the manufacturer's instruction. Immunoreactivity was evaluated by determining the percentage of cells expressing dUTPase in the examined fields, graded as low (0–50%) or high (> 50%). The PCNA index was evaluated as described previously (19).

Statistical analysis

Student's *t*-test was used to determine the statistical significance of the differences in cell viability between the two groups. The Mann–Whitney *U*-test was used for the analysis of gene expression between chronic liver disease (CLD) and HCC tissues. The χ^2-test was used to evaluate the correlation between clinicopathological characteristics and dUTPase expression status. Univariate and multivariate Cox proportional hazards regression analysis was used to evaluate the association of dUTPase expression and clinicopathological parameters with patient outcome. All statistical analyses were performed using SPSS software (SPSS software package; SPSS Inc., Chicago, IL, USA) and GRAPHPAD PRISM software (GraphPad Software Inc., La Jolla, CA, USA).

Results

Gene expression profiling identified the overexpression of *DUT* in hepatocellular carcinoma

To overcome the considerable individual variability of transcriptomic characteristics, we constructed a SAGE library of normal human liver using RNAs derived from five normal liver tissues. In addition, we constructed two SAGE libraries derived from three HCC tissues or corresponding non-cancerous liver tissues from patients who developed HCC with a history of chronic hepatitis C. We detected a total of 226 267 tags corresponding to 45 746 unique tags from these SAGE libraries (supporting information Table S1). After excluding the tags detected only once in each library, we selected 15 333 reliable unique transcripts expressed in at least one of the SAGE libraries to avoid contamination of tags derived from sequence errors. Then, we annotated these transcripts using SAGE Genie database and the Source database to identify the potential subcellular localization of transcripts categorized into eight groups in each SAGE library.

The number of nuclear component-related transcripts was increased in the HCC library compared with the normal liver and non-cancerous liver libraries, whereas the other cellular component-related transcripts did not show this tendency (supporting information Fig. S1). Because nuclear component-related genes may closely correlate with cancer cell proliferation and chemosensitivity (24), we further investigated the expression of nuclear component-related tags in each library, and identified 10 transcripts associated with nucleotide/nucleoside metabolism that are overexpressed in HCC (Table 1). Using Monte Carlo simulation, we evaluated the significance of differentially expressed transcripts in HCC and corresponding CLD libraries or in HCC and normal liver libraries. We identified a *DUT* gene encoding dUTPase (dUTPase) whose expression was significantly altered ($P = 0.01$). We also identified a *TS* gene encoding thymidylate synthase in the list, but the difference did not reach statistical significance.

dUTPase is a phosphatase known to maintain a dUMP pool by catalysing the hydrolysis of dUTP to dUMP, and thus provides a substrate of thymidylate synthase. Its role in HCC is unknown; therefore, we examined *DUT* expression in 20 independent HCC and corresponding non-cancerous liver tissues, and identified significant overexpression of *DUT* in HCC tissue ($P = 0.0015$) (Fig. 1A). Moreover, we detected more than a two-fold increase in *DUT* expression in 70% of HBV-related and HCV-related HCC cases (14 of 20 HCCs) compared with the non-cancerous liver tissues (Fig. 1B). We further examined the expression of *DUT* in 238 HCC tissues compared with the non-cancerous liver tissues using publicly available microarray data (GSE5975) (Fig. S2). Consistent with the SAGE data, *DUT* was overexpressed more than two-fold in 121 of 238 HCC tissues (median: 2.03), whereas *TS* was overexpressed more than two-fold in 54 of 238 HCC tissues (median: 1.41) compared with the non-cancerous liver tissues.

Pivotal role of dUTP pyrophosphatase expression in cell proliferation in hepatocellular carcinoma cell lines

In general, cancer gene signatures discovered by comparison between tumour and non-tumour tissues are more likely to reflect the differences in the control of cell proliferation and growth (25). Accordingly, we investigated the function of dUTPase in cell proliferation in HuH7 cells by *DUT* gene knockdown. *DUT* expression was decreased by 60–70% following the transfection of the siRNA constructs specifically targeting *DUT* 48 h after transfection (DUT1 in Fig. 2A and DUT2 in Fig. S3A), and cell growth was significantly inhibited compared with the control 72 h after transfection (Fig. 2B and Fig. S3B). Anchorage-independent cell growth was also significantly impaired by *DUT* gene knockdown 14 days after transfection (Fig. 2C). Furthermore, *DUT* gene knockdown decreased the numbers of both migrating and invading cells 72 h after transfection (Fig. 2D and E).

dUTPase is known to be associated with thymidylate synthesis (26), and thus we evaluated the effects of 5-FU, a thymidylate synthase inhibitor, on dUTPase expression in HCC cell lines *in vitro*. When we treated HuH7 cells with low-dose 5-FU (0.25 mg/ml), we could not detect any growth-inhibitory effects (Fig. 2F). Based on this condition, we evaluated the effect of *DUT* gene knockdown on 5-FU sensitivity 72 h after transfection.

Table 1. Genes associated with nucleic acid metabolism overexpressed in hepatocellular carcinoma

Tag sequence	Normal liver	Non-cancerous liver	HCC	Fold*	Gene	*P*-value†
CAGCTCCGCT	0	2	11	5.5	dUTP pyrophosphatase	0.010
AAAGGATAAT	0	0	3	> 3	General transcription factor II H, polypeptide 2	0.127
ACGGTCCAGG	0	0	3	> 3	Cytidine deaminase	0.127
ATGTAGAGTG	0	0	3	> 3	Thymidylate synthase	0.127
TGGGGATTAC	1	0	3	> 3	Zinc ribbon domain containing, 1	0.127
CACCCTGTAC	2	2	6	3	Solute carrier family 29	0.147
GAACGCCTAA	1	1	3	3	Dihydropyrimidinase-like 2	0.308
GCGCTGGTAC	0	1	3	3	2′-5′-oligoadenylate synthetase 3	0.308
CTTAGTGCAA	0	2	4	2	3′-phosphoadenosine 5′-phosphosulphate synthase 2	0.335
TTGTTACATC	0	2	3	1.5	Phosphoribosyl pyrophosphatase synthetase-associated protein 1	0.506

*Fold increase was calculated by dividing the number of tags in HCC by that of tags in non-cancerous liver. To avoid division by 0, a tag value of 1 was used for any tag that was not detectable in one sample.

†Statistical significance of differentially expressed genes between two groups (HCC and non-cancerous liver libraries) was calculated using Monte Carlo simulation.

HCC, hepatocellular carcinoma.

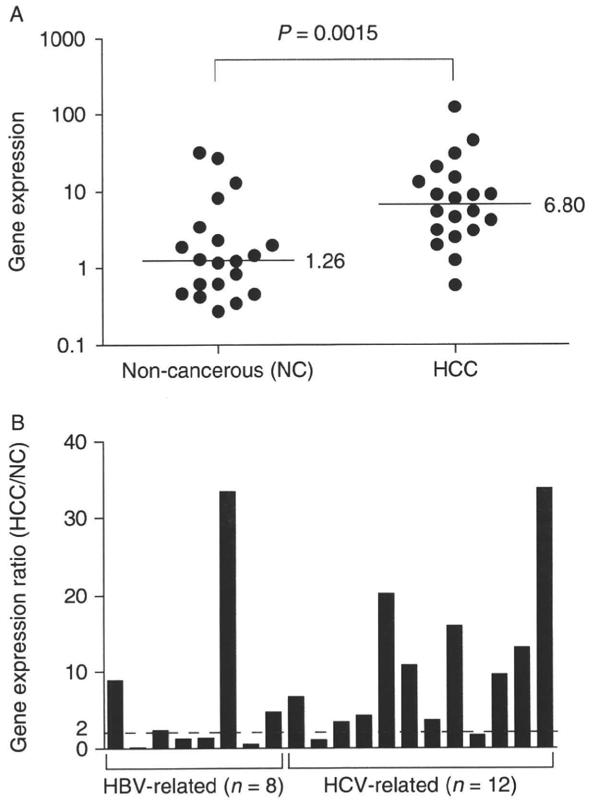

Fig. 1. (A) Quantitative reverse transcription-polymerase chain reaction analysis of *DUT* expression in hepatocellular carcinoma (HCC) and corresponding non-cancerous liver tissues. *DUT* was significantly activated in HCC tissues compared with non-cancerous liver tissues ($P = 0.0015$). A median value in each group is indicated. (B) *DUT* gene expression ratios of HCC and corresponding non-cancerous liver tissues. Fourteen of 20 HCC tissues expressed *DUT* more than two-fold compared with the background non-cancerous liver tissues. HBV, hepatitis B virus; HCV, hepatitis C virus.

Interestingly, *DUT* gene knockdown not only suppressed cell proliferation but also sensitized HuH7 cells to low-dose 5-FU (Fig. 2F and Fig. S3B). These data suggest that dUTPase overexpression in HCC tissues may be associated with enhanced cell proliferation and 5-FU resistance.

Intense dUTP pyrophosphatase expression is correlated with a poor prognosis in hepatocellular carcinoma patients

To characterize the clinicopathological characteristics of dUTPase expression in HCC, we performed IHC using an additional independent HCC cohort. Accordingly, we explored the dUTPase expression in HCC using 82 formalin-fixed paraffin-embedded HCC specimens. All HCC tissues were surgically resected at the Liver Disease Center of Kanazawa University Hospital with full clinical information, and their immunoreactivity to anti-dUTPase antibodies was evaluated by IHC. We noticed that anti-dUTPase antibodies reacted to both nuclear (red arrows) and cytoplasmic (blue arrows) isoforms of dUTPase, as described previously (26) (Fig. 3A and B). We therefore evaluated the nuclear and cytoplasmic expression of dUTPase separately. We stratified HCC tissues and evaluated the dUTPase expression status based on the percentages of dUTPase-positive cells. The frequency of nuclear or cytoplasmic dUTPase-positive cells was highly variable in each HCC tissue, and we defined HCCs with nuclear or cytoplasmic dUTPase expressed in ≥50% of tumour cells as nuclear or cytoplasmic dUTPase-high HCC (Fig. 3C). Nuclear dUTPase overexpression was detected in 36.6% (30 of 82), whereas cytoplasmic dUTPase overexpression was detected in 67.1% (55 of 82) of HCC tissues compared with the corresponding non-cancerous liver tissues

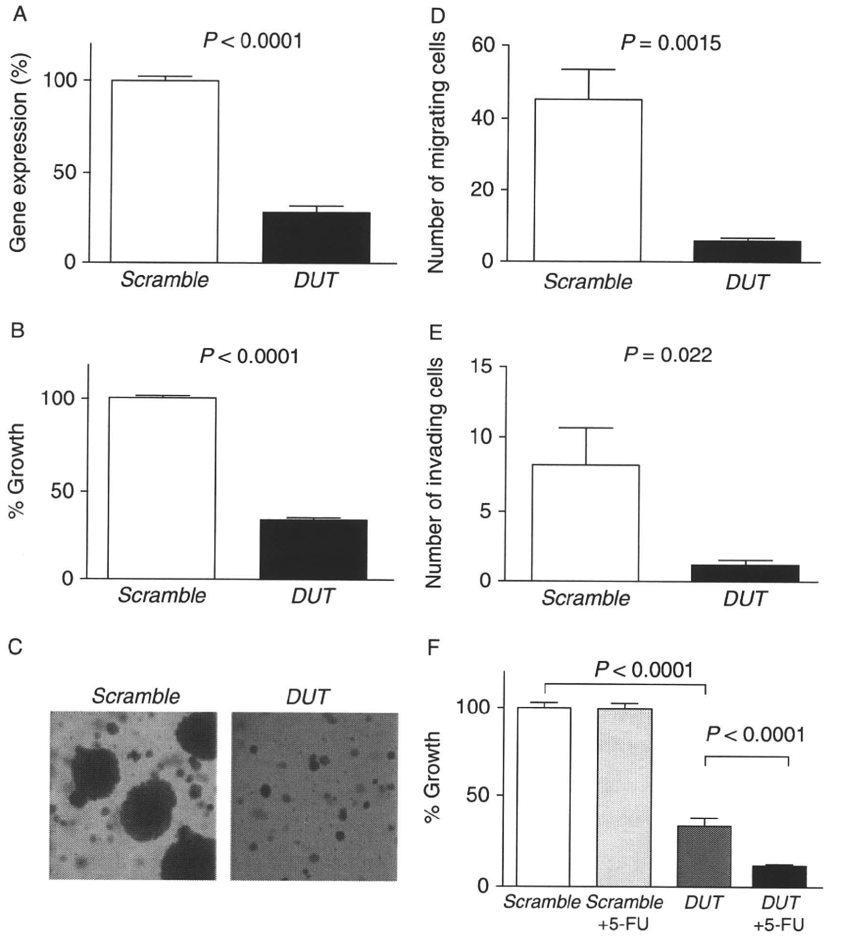

Fig. 2. (A) Transfection of small interfering RNAs targeting *DUT* (DUT1) decreased *DUT* expression compared with the control (scrambled sequence). Gene expression was evaluated in triplicate 72 h after transfection (mean ± SD). (B) *DUT* gene knockdown significantly suppressed cell proliferation ($P < 0.0001$). Cell viability was evaluated in triplicate 72 h after transfection (mean ± SD). (C) Soft agar assay. *DUT* gene knockdown suppressed anchorage-independent cell growth. (D and E) Matrigel invasion assay. *DUT* gene knockdown decreased the numbers of both migrating and invading cells. Experiments were performed in triplicate (mean ± SD). (F) *DUT* gene knockdown sensitized HuH7 cells to low-dose 5-fluorouracil (5-FU) (0.25 μg/ml), which had no effect on the cell proliferation in the control (mean ± SD).

(Table 2). In general, non-cancerous hepatocytes rarely expressed nuclear dUTPase (Fig. 3A).

We investigated the clinicopathological characteristics of nuclear or cytoplasmic dUTPase in low /high HCC cases (Table 2). The expression status of nuclear dUTPase showed no correlation with age, gender, virus, presence of cirrhosis, α-fetoprotein value, tumour size and TNM stages. However, nuclear dUTPase expression was significantly correlated with the histological grades of HCC ($P = 0.0099$), and high frequencies of nuclear dUTPase-positive cells were associated with poorly differentiated cell morphology in the HCC tissue. In contrast, cytoplasmic dUTPase expression was not correlated with the histological grades of HCC ($P = 0.077$). We examined the cell proliferation of these HCC samples by PCNA staining, and PCNA indexes were significantly higher in nuclear dUTPase high HCC than low HCC with statistical significance ($P = 0.01$) (Fig. S4).

We further investigated the prognostic significance of dUTPase expression in HCC. Strikingly, high nuclear dUTPase expression in HCC tissue correlated with a poor survival outcome compared with low nuclear dUTPase expression ($P = 0.0036$), whereas high cytoplasmic dUTPase expression had little effects when evaluated by recurrence-free survival (Fig. 3D). Furthermore, univariate Cox regression analysis showed a significant correlation between high nuclear dUTPase expression and a high risk of mortality (HR, 2.47; 95% CI, 1.08–5.66; $P = 0.032$; Table 3). By multivariate Cox regression analysis, TNM stage (HR, 2.75; 95% CI, 1.11–6.79; $P = 0.027$) and nuclear dUTPase (HR, 2.61; 95% CI, 1.13–6.05; $P = 0.024$) were independent prognostic factors associated with a high risk of mortality, and other clinicopathological features did not add independent prognostic information. These data indicate a significant correlation between the malignant potential of

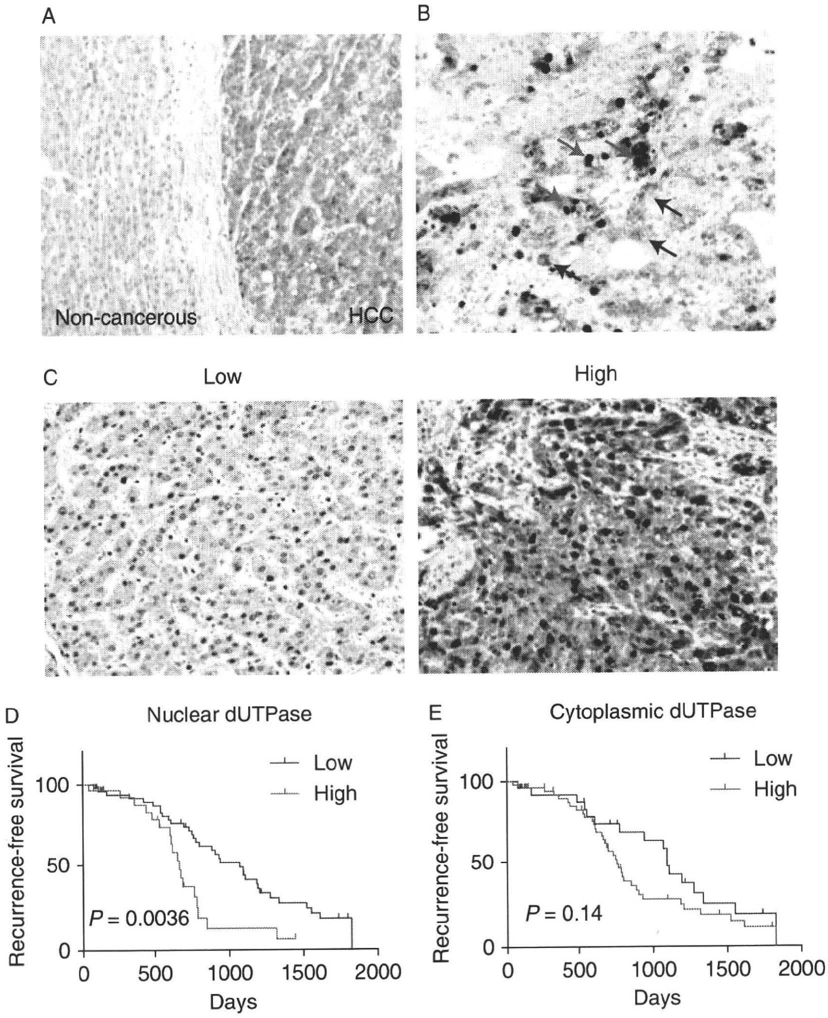

Fig. 3. Immunohistochemistry analysis of dUTP pyrophosphatase (dUTPase) expression in hepatocellular carcinoma (HCC). (A) A representative photomicrograph of dUTPase staining in an HCC and adjacent non-cancerous liver tissue. (B) A representative photomicrograph of dUTPase staining in an HCC. Both nuclear (red arrows) and cytoplasmic (blue arrows) forms of dUTPase were detected. (C) Representative photomicrographs of HCC tissues with low (0–50%) and high ($\geq$50%) frequencies of nuclear and cytoplasmic dUTPase-positive cells. (D and E) Kaplan–Meier survival analysis of HCC tissues with nuclear (D) or cytoplasmic (E) dUTPase expression. High percentages of nuclear dUTPase-positive tumour cells significantly correlated with poor clinical outcome in recurrence-free survival.

HCC and nuclear dUTPase expression, implicating the potential effectiveness of nuclear dUTPase level as a biomarker for predicting the survival of HCC patients after surgical resection.

Discussion

Here, using a global gene expression profiling approach (18), we have identified the activation of the nucleotide/nucleoside metabolism-related gene *DUT* (encoding dUTPase) in HCC. Notably, an intense dUTPase expression was detected in a subset of HCC with a poor prognosis. To the best of our knowledge, this is the first report describing the correlation between dUTPase activation and poor survival outcome in HCC patients.

In normal cells, dUTPase is known to catalyse the hydrolysis of dUTP to dUMP in order to maintain the dUMP pool at a certain level for thymidylate synthesis (26). Interestingly, dUTPase mutations in *Escherichia coli* increased dUTP levels, leading to dUTP misincorporation into DNA during replication, which resulted in DNA fragmentation and apoptosis (27). Furthermore, introduction of *E. coli* dUTPase into human tumour cells resulted in the induction of resistance to fluorodeoxyuridine cytotoxicity (28), suggesting a pivotal role of dUTPase in the prevention of DNA damage. Thus, dUTPase activation in the nucleus appears to be critical

Table 2. Clinicopathological characteristics and dUTP pyrophosphatase expression in hepatocellular carcinoma ($n = 82$)

dUTPase expression (nuclear)	Low ($n = 52$)	High ($n = 30$)	*P*-value
Age (< 60 years/≥60 years)	19/33	8/22	0.36
Sex (male/female)	36/16	23/7	0.47
Virus (HBV/HCV/B+C/NBNC)	15/33/1/3	10/20/0/0	0.48
Cirrhosis (yes/no)	33/19	22/8	0.36
AFP (< 20 ng/ml/≥20 ng/ml)	32/20	15/15	0.31
Histological grade*			
I–II	14	3	
II–III	36	20	
III–IV	2	7	0.0099
Tumour size (< 3 cm/≥3 cm)	31/21	19/11	0.74
TNM classification† (I, II/III, IV)	43/9	25/5	0.94

dUTPase expression (cytoplasmic)	Low ($n = 27$)	High ($n = 55$)	*P*-value
Age (< 60 years/≥60 years)	10/17	17/38	0.58
Sex (male/female)	19/8	40/15	0.82
Virus (HBV/HCV/B+C/NBNC)	8/17/1/1	17/36/0/2	0.56
Cirrhosis (yes/no)	17/10	38/17	0.58
AFP (< 20 ng/ml/≥20 ng/ml)	16/11	31/24	0.80
Histological grade*			
I–II	7	10	
II–III	20	36	
III–IV	0	9	0.077
Tumour size (< 3cm/≥3 cm)	17/10	33/22	0.80
TNM classification† (I, II/III, IV)	21/6	47/8	0.39

*Edmondson–Steiner grades.
†UICC TNM classification of liver cancer, 6th edition (2002).
AFP, α-fetoprotein; dUTPase, dUTP pyrophosphatase; HBV, hepatitis B virus; HCV, hepatitis C virus.

Table 3. Cox regression analysis of recurrence-free survival rate relative to dUTP pyrophosphatase expression and clinicopathological parameters ($n = 82$)

	Univariate		Multivariate	
Variables (n)	HR (95% CI)	*P*-value	HR (95% CI)	*P*-value
Child–Pugh				
A	1			
B	1.73 (0.50–5.97)	0.38		
Tumour size				
< 3 cm ($n = 50$)	1			
≥3 cm ($n = 32$)	1.58 (0.69–3.63)	0.28		
TNM stage*				
I, II ($n = 68$)	1		1	
III, IV ($n = 14$)	2.57 (1.05–6.29)	0.039	2.75 (1.11–6.79)	0.027
Serum AFP				
< 20 ng/ml ($n = 49$)	1			
≥20 ng/ml ($n = 38$)	1.54 (0.66–3.56)	0.31		
Microvascular invasion				
No	1			
Yes	1.98 (0.89–4.44)	0.095		
BCLC stage				
A	1			
B/C	2.16 (0.93–5.00)	0.07		
Cytoplasmic dUTPase				
Low ($n = 27$)	1			
High ($n = 55$)	1.15 (0.50–2.62)	0.73		
Nuclear dUTPase				
Low ($n = 52$)	1		1	
High ($n = 30$)	2.47 (1.08–5.66)	0.032	2.61 (1.13–6.05)	0.024

*UICC TNM classification of liver cancer, 6th edition (2002).
AFP, α-fetoprotein; CI, confidence intervals; dUTPase, dUTP pyrophosphatase; HR, hazard ratio.

for preventing DNA damage possibly at the S phase. Specifically, this activation may prevent dUTP misincorporation in various cancers and thus avert DNA damage and apoptosis induction. Indeed, dUTPase activation has recently been reported in colorectal and brain cancer (29, 30), and dUTPase accumulation might correlate with 5-FU-based chemotherapy resistance and poor prognosis in colorectal cancer (26).

If dUTPase activation plays a central role in the development of resistance to thymidylate synthase inhibitors in order to prevent a DNA damage response, dUTPase inhibition may facilitate the eradication of cancer cells by sensitizing these cells to such inhibitors. Indeed, a recent study suggested a drastic sensitization of colon cancer cells to 5-FU by siRNAs-mediated dUTPase suppression (31, 32), which is consistent with our current observation. Because all HCC samples used in this study were surgically resected, we could not evaluate the effect of dUTPase expression on clinical HCC patients' outcome in relation to chemosensitivity to thymidylate synthase inhibitors. Nevertheless, intense nuclear dUTPase expression may be a good biomarker for predicting the response to thymidylate synthase inhibitors, and its usefulness should be further evaluated in the future.

In conclusion, comprehensive gene expression profiling shed new light on the role of dUTPase in HCC. Nuclear dUTPase accumulation is potentially a good biomarker for predicting poor prognosis in HCC patients, and the development of a dUTPase inhibitor may promote the possibility of tumour eradication in HCC patients.

Acknowledgements

The authors would like to thank Ms Masayo Baba and Nami Nishiyama for technical assistance. This research was supported in part by a Grant-in-Aid for Special Purposes from the Ministry of Education, Culture, Sports, Science and Technology, Japan (no. 20599005).

Grant support: Grant-in-Aid for Special Purposes from the Ministry of Education, Culture, Sports, Science and Technology, Japan (no. 20599005).

References

1. Parkin DM, Bray F, Ferlay J, Pisani P. Global cancer statistics, 2002. *CA Cancer J Clin* 2005; **55**: 74–108.
2. El-Serag HB, Rudolph KL. Hepatocellular carcinoma: epidemiology and molecular carcinogenesis. *Gastroenterology* 2007; **132**: 2557–76.
3. Farazi PA, Depinho RA. Hepatocellular carcinoma pathogenesis: from genes to environment. *Nat Rev Cancer* 2006; **6**: 674–87.
4. Roessler S, Budhu A, Wang XW. Future of molecular profiling of human hepatocellular carcinoma. *Future Oncol* 2007; **3**: 429–39.
5. El-Serag HB, Marrero JA, Rudolph L, Reddy KR. Diagnosis and treatment of hepatocellular carcinoma. *Gastroenterology* 2008; **134**: 1752–63.
6. Llovet JM, Bruix J. Novel advancements in the management of hepatocellular carcinoma in 2008. *J Hepatol* 2008; **48**(Suppl. 1): S20–37.
7. Poon RT, Fan ST, Lo CM, Liu CL, Wong J. Long-term survival and pattern of recurrence after resection of small hepatocellular carcinoma in patients with preserved liver function: implications for a strategy of salvage transplantation. *Ann Surg* 2002; **235**: 373–82.
8. Friedman MA. Primary hepatocellular cancer–present results and future prospects. *Int J Radiat Oncol Biol Phys* 1983; **9**: 1841–50.
9. Lin DY, Lin SM, Liaw YF. Non-surgical treatment of hepatocellular carcinoma. *J Gastroenterol Hepatol* 1997; **12**: S319–28.
10. Nagano H, Miyamoto A, Wada H, *et al.* Interferon-alpha and 5-fluorouracil combination therapy after palliative hepatic resection in patients with advanced hepatocellular carcinoma, portal venous tumor thrombus in the major trunk, and multiple nodules. *Cancer* 2007; **110**: 2493–501.
11. Patt YZ, Hassan MM, Lozano RD, *et al.* Phase II trial of systemic continuous fluorouracil and subcutaneous recombinant interferon alfa-2b for treatment of hepatocellular carcinoma. *J Clin Oncol* 2003; **21**: 421–7.
12. Urabe T, Kaneko S, Matsushita E, Unoura M, Kobayashi K. Clinical pilot study of intrahepatic arterial chemotherapy with methotrexate, 5-fluorouracil, cisplatin and subcutaneous interferon-alpha-2b for patients with locally advanced hepatocellular carcinoma. *Oncology* 1998; **55**: 39–47.
13. Obi S, Yoshida H, Toune R, *et al.* Combination therapy of intraarterial 5-fluorouracil and systemic interferon-alpha for advanced hepatocellular carcinoma with portal venous invasion. *Cancer* 2006; **106**: 1990–7.
14. Honda M, Yamashita T, Ueda T, *et al.* Different signaling pathways in the livers of patients with chronic hepatitis B or chronic hepatitis C. *Hepatology* 2006; **44**: 1122–38.
15. Nishino R, Honda M, Yamashita T, *et al.* Identification of novel candidate tumour marker genes for intrahepatic cholangiocarcinoma. *J Hepatol* 2008; **49**: 207–16.
16. Yamashita T, Honda M, Takatori H, *et al.* Genome-wide transcriptome mapping analysis identifies organ-specific gene expression patterns along human chromosomes. *Genomics* 2004; **84**: 867–75.
17. Yamashita T, Kaneko S, Hashimoto S, *et al.* Serial analysis of gene expression in chronic hepatitis C and hepatocellular carcinoma. *Biochem Biophys Res Commun* 2001; **282**: 647–54.
18. Yamashita T, Honda M, Kaneko S. Application of serial analysis of gene expression in cancer research. *Curr Pharm Biotechnol* 2008; **9**: 375–82.
19. Yamashita T, Honda M, Takatori H, *et al.* Activation of lipogenic pathway correlates with cell proliferation and poor prognosis in hepatocellular carcinoma. *J Hepatol* 2009; **50**: 100–10.
20. Velculescu VE, Zhang L, Vogelstein B, Kinzler KW. Serial analysis of gene expression. *Science* 1995; **270**: 484–7.
21. Yamashita T, Hashimoto S, Kaneko S, *et al.* Comprehensive gene expression profile of a normal human liver. *Biochem Biophys Res Commun* 2000; **269**: 110–6.
22. Polyak K, Xia Y, Zweier JL, Kinzler KW, Vogelstein B. A model for p53-induced apoptosis. *Nature* 1997; **389**: 300–5.
23. Misu H, Takamura T, Matsuzawa N, *et al.* Genes involved in oxidative phosphorylation are coordinately upregulated with fasting hyperglycaemia in livers of patients with type 2 diabetes. *Diabetologia* 2007; **50**: 268–77.
24. Longley DB, Harkin DP, Johnston PG. 5-fluorouracil: mechanisms of action and clinical strategies. *Nat Rev Cancer* 2003; **3**: 330–8.
25. Whitfield ML, George LK, Grant GD, Perou CM. Common markers of proliferation. *Nat Rev Cancer* 2006; **6**: 99–106.
26. Ladner RD, Lynch FJ, Groshen S, *et al.* dUTP nucleotidohydrolase isoform expression in normal and neoplastic tissues: association with survival and response to 5-fluorouracil in colorectal cancer. *Cancer Res* 2000; **60**: 3493–503.
27. El-Hajj HH, Zhang H, Weiss B. Lethality of a dut (deoxyuridine triphosphatase) mutation in *Escherichia coli*. *J Bacteriol* 1988; **170**: 1069–75.
28. Canman CE, Radany EH, Parsels LA, *et al.* Induction of resistance to fluorodeoxyuridine cytotoxicity and DNA damage in human tumor cells by expression of *Escherichia coli* deoxyuridinetriphosphatase. *Cancer Res* 1994; **54**: 2296–8.
29. Fleischmann J, Kremmer E, Muller S, *et al.* Expression of deoxyuridine triphosphatase (dUTPase) in colorectal tumours. *Int J Cancer* 1999; **84**: 614–7.
30. Romeike BF, Bockeler A, Kremmer E, *et al.* Immunohistochemical detection of dUTPase in intracranial tumors. *Pathol Res Pract* 2005; **201**: 727–32.
31. Koehler SE, Ladner RD. Small interfering RNA-mediated suppression of dUTPase sensitizes cancer cell lines to thymidylate synthase inhibition. *Mol Pharmacol* 2004; **66**: 620–6.

32. Wilson PM, Fazzone W, Labonte MJ, *et al.* Novel opportunities for thymidylate metabolism as a therapeutic target. *Mol Cancer Ther* 2008; **7**: 3029–37.

Supporting Information

Additional Supporting Information may be found in the online version of this article:

Fig. S1. Subcellular localization of genes detected in each SAGE library.

Fig. S2. Microarray analysis of *DUT* and *TS* gene expression in 238 HCC cases publicly available (GSE5975). *DUT* was overexpressed more than 2-fold in 121 of 238 HCC tissues (median: 2.03), whereas *TS* was overexpressed more than 2-fold in 54 of 238 HCC tissues (median: 1.41) compared with the non-cancerous liver tissues.

Fig. S3. (A) Transfection of siRNAs targeting *DUT* (DUT2) decreased *DUT* expression compared with the control (scrambled sequence). Gene expression was evaluated in triplicates 72 hours after transfection (mean $\pm$ SD). (B) *DUT* gene knockdown sensitized HuH7 cells to low-dose 5-FU (0.25 mg/ml) (mean $\pm$ SD).

Fig. S4. Nuclear and cytoplasmic dUTPase expression and cell proliferation in HCC. PCNA indexes in nuclear dUTPase-high HCC were higher than those in -low HCC with statistical significance (P = 0.01). Cytoplasmic dUTPase expression was not associated with PCNA indexes in HCC.

Table S1. A summary of constructed SAGE libraries.

Please note: Wiley-Blackwell is not responsible for the content or functionality of any supporting materials supplied by the authors. Any queries (other than missing material) should be directed to the corresponding author for the article.

ORIGINAL ARTICLE

CD14$^+$ Monocytes Are Vulnerable and Functionally Impaired Under Endoplasmic Reticulum Stress in Patients With Type 2 Diabetes

Takuya Komura,[1] Yoshio Sakai,[1] Masao Honda,[1] Toshinari Takamura,[1] Kouji Matsushima,[2] and Shuichi Kaneko[1]

OBJECTIVE—Although patients with diabetes suffer from increased infections and a higher incidence of cancer due to impaired immune function, details on diabetes-induced decrease in immunity are lacking. We assessed how immune-mediating peripheral blood mononuclear cells (PBMCs) are affected in diabetes.

RESEARCH DESIGN AND METHODS—From 33 patients with type 2 diabetes and 28 healthy volunteers, we obtained PBMCs and investigated their susceptibility to apoptosis and functional alteration.

RESULTS—In a subpopulation of PBMCs, monocytes derived from patients with diabetes were more susceptible to apoptosis than monocytes from healthy volunteers. Monocytes from patients with diabetes had decreased phagocytotic activity and were less responsive to Toll-like receptor (TLR) ligands, although the expression of TLRs did not differ significantly between the two groups. Furthermore, monocytes from patients with diabetes had a distinctly different gene expression profile compared with monocytes from normal volunteers as assessed with DNA microarray analysis. Specifically, quantitative real-time detection PCR measurements showed an elevated expression of the markers of endoplasmic reticulum (ER) stress in diabetic monocytes, and electron microscopic examination of monocytes revealed morphologic alterations in the ER of cells derived from patients with diabetes. Consistently, the ER stress inducer tunicamycin increased apoptosis of otherwise healthy monocytes and attenuated the proinflammatory responses to TLR ligands.

CONCLUSIONS—These data suggest that monocytes comprise a substantially impaired subpopulation of PBMCs in patients with diabetes and that ER stress is involved in these pathologic changes mechanistically. This implies that the affected monocytes should be investigated further to better understand diabetic immunity. ***Diabetes* 59:634–643, 2010**

From [1]Disease Control and Homeostasis, Kanazawa University, Graduate School of Medical Science, Kanazawa, Japan; and the [2]Department of Molecular Preventive Medicine, School of Medicine, The University of Tokyo, Tokyo, Japan.
Corresponding author: Shuichi Kaneko, skaneko@m-kanazawa.jp.
Received 13 May 2009 and accepted 16 November 2009. Published ahead of print at http://diabetes.diabetesjournals.org on 3 December 2009. DOI: 10.2337/db09-0659.

Type 2 diabetes is the most frequent metabolic disease and the leading cause of human morbidity and mortality (1,2). Based on epidemiologic data, patients with diabetes are immunocompromised and have an increased incidence of infections in the respiratory tract, urinary tract, and skin (3–5). The high incidence of colorectal, breast, and pancreatic malignancies in patients with diabetes is also considered to be a consequence of diabetes-associated defects in immune function (6,7).

Although studies on immune cells and circulating cytokines have shed some light on this diabetic immunologic phenomenon, conflicting results have been reported and do not adequately explain the perturbed immune function in patients with diabetes. Controversial results concerning the phagocytotic activity of polymorphonuclear neutrophils and monocytes are in part due to differences in the patients themselves, insufficient numbers in the study populations, or inconsistencies in the collection of the cell populations under investigation (8–11). Therefore, further studies are needed to explain the decreased immune function of patients with diabetes.

We previously investigated the gene expression signatures of peripheral blood mononuclear cells (PBMCs) in patients with diabetes and observed transcriptional expression features that were distinct from those of healthy volunteers (12). Apoptosis-related genes were upregulated in the PBMCs of patients with diabetes. Based on this result, we investigated apoptotic activity and immunologic function in PBMCs from patients with type 2 diabetes.

We observed that the CD14$^+$ monocyte fraction was the most affected subpopulation of PBMCs from these patients; these cells were especially vulnerable to apoptosis compared with other cell subpopulations. We also found that CD14$^+$ monocytes demonstrated attenuated phagocytotic activity and deficient Toll-like receptor (TLR) signaling, both of which are important for innate immunity (13,14). Transcriptional analysis and electron microscopic examination of monocytes from patients with diabetes showed evidence of endoplasmic reticulum (ER) stress, which may underlie the functional defects in these cells. Collectively, the data presented herein show that CD14$^+$ monocytes are a vulnerable cell population under ER stress in these patients that could contribute to decreases in immune function in diabetes.

RESEARCH DESIGN AND METHODS

Thirty-three patients with type 2 diabetes (male/female, 15/18; age 62.0 ± 8.6 years; A1C 9.2 ± 2.0%) and 28 healthy volunteers (male/female, 15/13; age 58.2 ± 10.2 years; A1C 5.4 ± 0.7%) were enrolled consecutively for the

TABLE 1
Characteristics of the study subjects

	Diabetic patients (n = 33)	Healthy volunteers (n = 28)	P
Age (years)	62.0 ± 8.6	58.2 ± 10.2	NS
Sex (male/female)	15/18	15/13	NS
BMI (kg/m^2)	23.5 ± 4.2	23.6 ± 4.8	NS
White blood cell counts (ml)	4,800 ± 1,700	5,600 ± 1,900	NS
Lymphocytes (%)	23.5 ± 3.5	22.7 ± 2.5	NS
Monocytes (%)	5.2 ± 1.6	6.1 ± 2.3	NS
Hemoglobin (g/dl)	14.1 ± 1.3	13.6 ± 1.6	NS
Total cholesterol (mg/dl)	182 ± 24	180 ± 35	NS
Triglyceride (mg/dl)	138 ± 37	163 ± 33	NS
FPG (mg/dl)	185 ± 38	86 ± 7.4	<0.001
A1C (%)	9.2 ± 2.0	5.4 ± 0.7	<0.001
Diabetic complications (+/−)*	19/14	NA	
Insulin treatment (+/−)	10/23	NA	

Data are means ± SD. *Diabetic complications: nephropathy, neuropathy, retinopathy, macroangiopathy. FPG, fasting plasma glucose; NA, not applicable.

apoptosis assay (Table 1). The groups were not significantly different in terms of their clinical parameters, except for the fasting plasma glucose and A1C levels. The patients with diabetes (n = 16) from whom adequate numbers of monocytes were obtained were enrolled for additional experiments along with 17 other patients with diabetes (male/female, 8/9; age 60.5 ± 7.2 years; A1C 8.8 ± 1.8%) whose clinical profiles fit the diabetic profile (Table 1). Informed consent for this study was obtained from all subjects. The experimental protocol was carried out in accordance with the Declaration of Helsinki.

Isolation of subpopulations of PBMCs and flow cytometric analysis. PBMCs were freshly isolated from heparinized venous blood using Ficoll-Hypaque (Sigma-Aldrich, St. Louis, MO) as previously described (12). CD4$^+$ T-cell and CD14$^+$ monocyte subpopulations were isolated using a magnetic cell sorting system in accordance with the manufacturer's protocol (Miltenyi Biotec, Bergisch Gladbach, Germany). Isolated cells were purified by >90% as measured by flow cytometric analysis using FACSCalibur flow cytometer (BD Biosciences, San Jose, CA). To assess the expression of TLRs on monocytes, PBMCs were incubated with phosphatidylethanolamine (PE)-labeled anti-TLR2, -TLR3, or -TLR4 (eBioscience, San Diego, CA) and fluorescein isothiocyanate (FITC)-labeled anti-CD14 antibodies (BD Biosciences) and analyzed by flow cytometry. Data were analyzed using CELLQuest Software (BD Biosciences).

Quantitative real-time detection PCR. Real-time detection (RTD)-PCR was performed as previously described (15). Briefly, total RNA obtained from cells using a MicroRNA isolation kit (Stratagene, La Jolla, CA) was reverse-transcribed using 1 μg oligo (dT) primer and Super Script II Reverse transcriptase (Invitrogen, Carlsbad, CA). The relative quantities of mRNA expression were analyzed by RTD-PCR using ABI PRISM 7900 HT Sequence Detection System (Applied Biosystems, Foster City, CA). All primer pairs and probes were obtained from the TaqMan assay reagents library. Expression levels of genes were calculated with the $2^{-\Delta\Delta Ct}$ method using either β-actin or GAPDH as internal control genes.

Apoptotic cell detection assay. Freshly isolated PBMCs were incubated with AIM-V (Invitrogen) serum-free culture media containing 5 or 30 mmol/l glucose at 37°C with 5% CO_2 for up to 24 h. The cells were incubated with FITC-labeled anti-CD4, -CD14, or -CD56 antibodies (BD Biosciences) and with PE-labeled annexin-V and 7-amino-actinomycin D (7-AAD) (BD Biosciences) in PBS containing 2% BSA (Sigma-Aldrich). Apoptotic cells were determined by flow cytometry as the fraction of cells labeled with annexin-V that were 7-AAD negative. At least 10,000 cells per sample were analyzed.

Phagocytosis assay. Phagocytotic activity was assessed using a Phagotest Kit (Orpegen Pharma, Heidelberg, Germany) and FITC-labeled opsonized *Escherichia coli* in accordance with the manufacturer's protocol. Briefly, heparinized whole blood obtained from the 33 patients with diabetes and 28 healthy volunteers was incubated with FITC-labeled *E. coli* for 10 min at 37°C. After removing the erythrocytes, the remaining cells were incubated with propidium iodide to detect viable leukocytes by flow cytometry. Monocyte populations were assessed based on cellular granularity and size as side scatter and forward scatter, respectively, and FITC-positive cells were assessed as monocytes with phagocytosed FITC-labeled *E. coli*.

TLR ligand stimuli and expression of proinflammatory cytokine genes. Peptidoglycan (PGN; 1 μg/ml) from *Streptomyces sp.* (Sigma-Aldrich), Poly (I:C) (5 μg/ml; Sigma-Aldrich), and lipopolysaccharide (LPS; 2 μg/ml) from *E. coli* (Sigma-Aldrich), which are TLR2, TLR3, and TLR4 ligands, respectively, were added to monocytes (3 × 10^5 cells) freshly isolated from the 33 patients and 28 healthy volunteers in AIM-V media. Before and 3 h after incubation, the expression of tumor necrosis factor-α (TNF-α) and interleukin-1β (IL-1β) was analyzed by RTD-PCR.

Analysis of gene expression by DNA microarray. Total RNA was obtained from CD14$^+$ monocytes using MicroRNA isolation kit (Stratagene), and the mRNA was amplified twice using the Amino Allyl MessageAmp aRNA Kit (Ambion, Austin, TX). The reference RNA sample was isolated from CD14$^+$ monocytes from a 30-year-old healthy male volunteer and amplified in the same manner. Amplified mRNA was labeled with cyanin (Cy) 5 or Cy3 (Amersham, Buckinghamshire, U.K.). Equal amounts of the amplified mRNAs were hybridized to an oligo-DNA chip (AceGene Human Oligo Chip 30K; Hitachi Software Engineering, Yokohama, Japan) overnight and washed prior to image scanning.

The fluorescence intensity of each spot on the oligo-DNA chip was obtained using cDNA Microarray Scan Array G (PerkinElmer, Wellesley, MA). The obtained images were quantified using DNAsis array V2.6 software (Hitachi Software Engineering). For normalization, the intensity of each spot with oligo DNA was subtracted from that of spots without oligo DNA in the same block. The spot was validated when the intensity was within the intensity plus or minus a twofold range of SD within each block. By calibrating the median as the base value, the intensities of all spots were adjusted for normalization between Cy5 and Cy3. Hierarchic clustering of gene expression was calibrated using the method described above using BRB Array Tools (http://linus.nci.nih.gov/BRB-ArrayTools.html). The nonfiltered data were log-transformed and applied to the average linkage clustering with centered correlation. For the functional analysis of the 813 upregulated genes, we used GenMAPP (http://www.genmapp.org), a computer program designed for viewing and analyzing genome-scale data on MAPPs representing biological pathways and any other groups of genes.

Electron microscopy. Monocytes obtained from three healthy volunteers and three patients with diabetes were fixed with 2.5% glutaraldehyde and then postfixed in 1% (vol/vol) cacodylate-buffered osmium tetroxide. Samples were dehydrated in a graded series of ethanol, transferred to propylene oxide, and embedded in Epon-Araldite (Sigma-Aldrich). Ultrathin sections were obtained and observed under a Hitachi H-7500 electron microscope (Hitachi High-Technologies, Hitachinaka, Japan).

Caspase-3 assay and enzyme-linked immunosorbent assay (ELISA) of cytokines. Monocytes from a healthy volunteer were harvested and treated with tunicamycin (1 or 5 μg/ml) in AIM-V media. Every 3 h up to 12 h after tunicamycin treatment, we assessed apoptosis by flow cytometry as described above. After 12 h of incubation, the expression levels of BCL-2, C/EBP homologous protein (CHOP), and BiP (immunoglobulin heavy chain binding protein) were assessed by RTD-PCR. The DEVD-cleaving activity of active caspase-3 was measured using labeled Asp-Glu-Val-Asp-p-nitroanilide (DEVD-pNA) as the substrate and the Caspase-3 Colorimetric Assay Kit (Promega, Madison, WI) in accordance the manufacturer's protocol. The pNA light emission was quantified using a microtiter plate reader at a wavelength of 405 nm. In addition, we measured the production of proinflammatory cytokines by RTD-PCR 6 h after treatment of monocytes (3 × 10^5 cells) with tunicamycin (1 or 5 μg/ml) or the TLR ligands PGN (1 μg/ml), Poly (I:C) (5 μg/ml), and LPS (2 μg/ml). The concentrations of TNF-α, IL-1β, and IL-6 in the culture supernatants were measured using an ELISA kit (eBioscience).

Statistical analysis. Data are expressed as means ± SEM. The Mann-Whitney U test was applied to assess the significant differences between the two groups. Statistical significance was determined as $P < 0.05$, $P < 0.01$, and $P < 0.001$.

RESULTS

Increased apoptosis of CD14$^+$ monocytes from patients with diabetes. We first assessed the frequency of apoptosis in the PBMC fractions from 33 patients with diabetes and 28 nondiabetic healthy volunteers. Apoptosis of the isolated cells was assessed after 3-h incubation in AIM-V serum-free media containing 5 mmol/l glucose (physiological concentration in blood). As shown in Fig. 1*A*, a significant difference in the frequency of apoptosis was observed in the PBMCs isolated from patients with diabetes and healthy volunteers. Adding serum to AIM-V serum-free media did not affect the difference in apoptosis (data

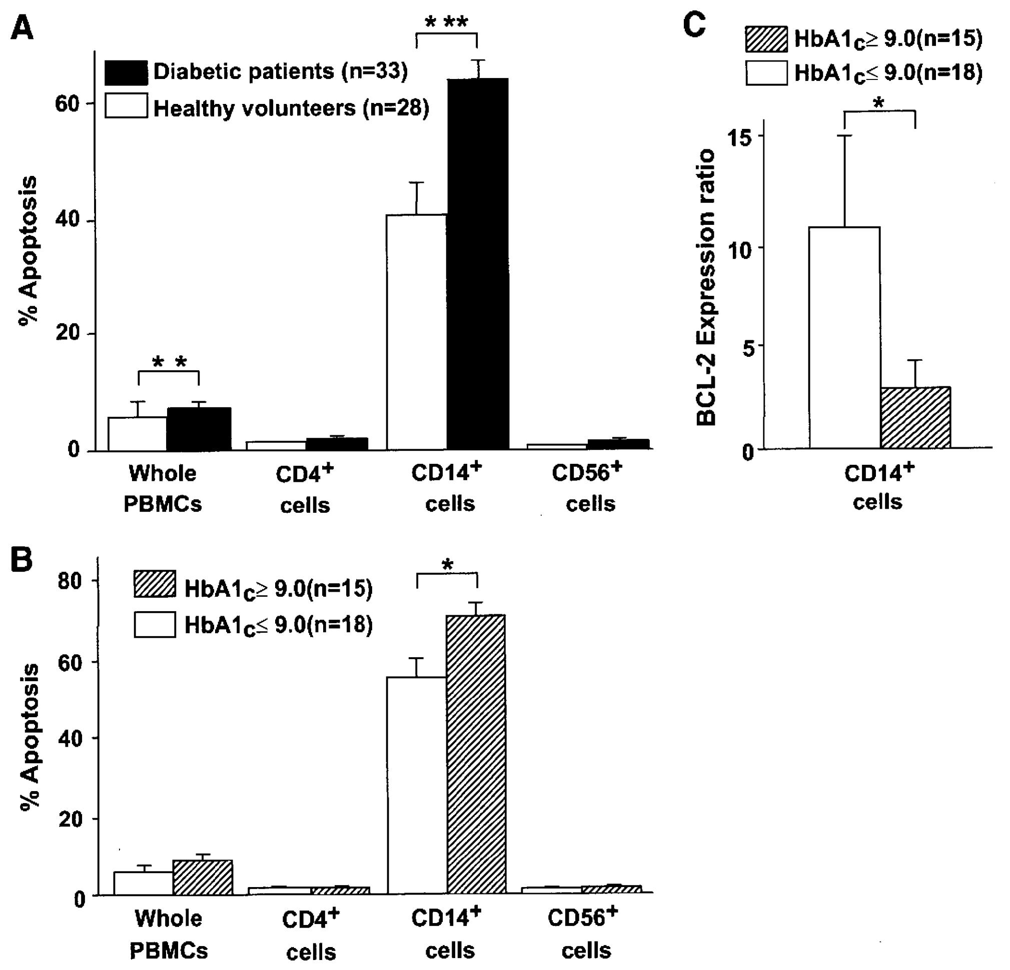

FIG. 1. Monocytes contributed to the vulnerability of the PBMCs in patients with diabetes. ***A*****: PBMCs were obtained from 33 patients with diabetes and 28 healthy volunteers. Isolated PBMCs were harvested in AIM-V serum-free culture media supplemented with 5 mmol/l glucose for 3 h and incubated with FITC-labeled anti-CD4, -CD14, or -CD56 antibodies, together with PE-labeled annexin-V to assess the frequency of apoptotic cells in each subpopulation of PBMCs. Apoptotic cells were identified by double-staining with PE-labeled annexin-V and 7-AAD by flow cytometry. The frequencies of apoptotic cells determined as the annexin-V–positive and 7-AAD–negative population are expressed as means ± SEM with statistical comparisons for both groups. The nonparametric Mann-Whitney** ***U*** **test was used to calculate the** ***P*** **value. $**P < 0.01$, $***P < 0.001$. The PBMCs of patients with diabetes were more susceptible to apoptosis than those of healthy volunteers, and $CD14^+$ monocytes were contributors.** ***B*****: Among the 33 patients with diabetes, those with poor glycemic control reflected as A1C ≥9.0% were more susceptible to apoptosis in $CD14^+$ monocytes. Data are expressed as means ± SEM with a statistical comparison of both groups. $*P < 0.05$.** ***C*****: Monocytes were isolated from 15 patients with A1C ≥9.0% and 18 patients with A1C <9.0%. The expression of the BCL-2 gene in their monocytes before and after incubation in AIM-V serum-free media was assessed by RTD-PCR. After 3-h incubation, the expression of BCL-2 was not upregulated in the poor glycemic control group (A1C ≥9.0%), compared with the fair control group (A1C <9.0%). Data are expressed as means ± SEM with statistical comparisons of both groups. $*P < 0.05$.**

not shown). The numbers of whole PBMCs and $CD4^+$, $CD14^+$, and $CD56^+$ cells were similar in both diabetic and healthy subjects (data not shown). $CD14^+$ monocytes were observed to be the major contributor to the increased apoptosis measured in the PBMCs. In contrast, apoptosis of $CD4^+$ T-cells and $CD56^+$ natural killer (NK) cells was not significantly different between the two groups (Fig. 1*A*). When the incubation period in culture media with or without serum was extended to 24 h, ~20% of the $CD56^+$ NK cells of both patients with diabetes and healthy volunteers were induced to undergo apoptosis. When incubation period was extended to 5 days, ~5% of $CD4^+$ T-cells of both patients with diabetes and healthy volunteers were induced to undergo apoptosis; there was no significant difference in cell viability of $CD56^+$ NK cells and $CD4^+$ T-cells between the two groups (data not shown). BCL-2 expression of $CD4^+$ T-cells was not different between the two groups (data not shown). Apoptosis of PBMC subpopulations incubated in culture media containing 30 mmol/l glucose was not different from cells incubated in 5 mmol/l glucose-containing media (data not shown). Moreover, the susceptibility of PBMCs from patients with diabetes to apoptosis was not related to clinical features such as vascular complications, insulin treatment, and fasting plasma glucose concentrations (data not shown).

However, among the 33 patients with diabetes, the frequency of apoptotic $CD14^+$ monocytes from those with poor glycemic control (A1C ≥9.0%) was elevated compared with patients with fair glycemic control (A1C <9.0%) (Fig. 1*B*). Furthermore, after 3-h incubation, the increased ratio of the expression of the antiapoptotic gene, BCL-2, was substantially lower in monocytes from the 15 patients with A1C ≥9.0% compared with the 18

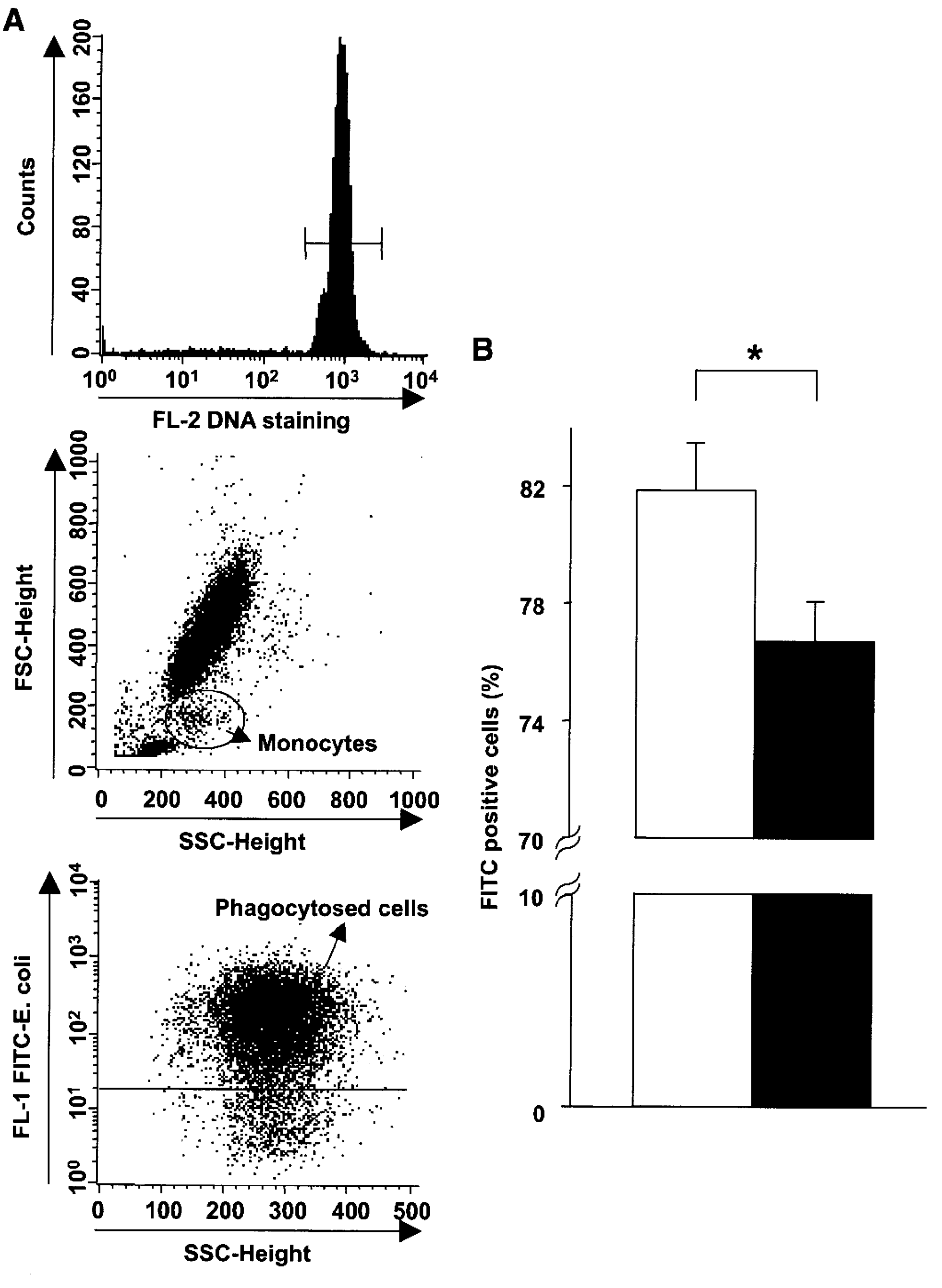

FIG. 2. Attenuated phagocytosis activity in diabetic monocytes. Whole PBMCs were incubated with FITC-labeled *E. coli* for 10 min followed by propidium iodide staining and flow cytometric analysis. *A*: Gated propidium iodide–positive populations were viable leukocyte populations (*upper panel*). The monocyte population was assessed using granularity (side scatter) and size (forward scatter) (*middle panel*). For the gated cells indicating viable monocytes, FITC-positive cells were assessed as monocytes containing phagocytosed FITC-labeled *E. coli* (*lower panel*). *B*: The frequency of monocytes containing phagocytosed *E. coli* in patients with diabetes (■, $n = 33$) was less than that in healthy volunteers (□, $n = 28$). Data are expressed as means ± SEM. *$P < 0.05$.

patients having A1C <9.0%, as assessed by RTD-PCR (Fig. 1*C*). These data suggest that the monocytes of patients with diabetes are susceptible to apoptosis, especially under conditions of poor glycemic control.

Attenuated function of monocytes from patients with diabetes. To determine whether functional alterations exist in monocytes isolated from the 33 patients with diabetes, we cocultured the monocytes with FITC-labeled *E. coli* and counted the number of fluorescent monocytes that phagocytosed the labeled *E. coli* by flow cytometry. The ratio of monocytes that phagocytosed *E. coli* to all monocytes in patients with diabetes was higher than in the healthy volunteers (Fig. 2*A* and *B*). No significant correlation was observed between the ratio of phagocy-

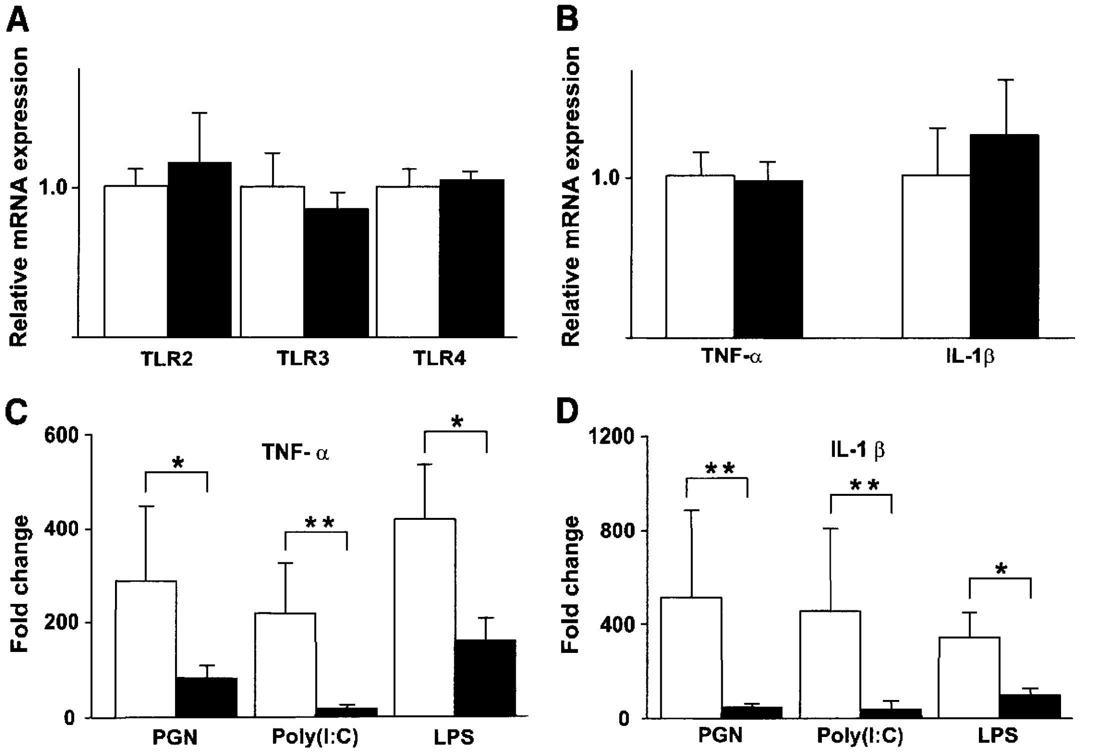

FIG. 3. Hyporesponsiveness to TLR ligand stimuli by the monocytes of patients with diabetes. ***A–D*: Isolated CD14$^+$ monocytes from 33 patients with diabetes (■) and 28 healthy volunteers (□) were cultured in AIM-V serum-free media supplemented with each TLR ligand: PGN, Poly (I:C), and LPS. After 3-h incubation, RNA was isolated from the monocytes, and the expression levels of the TNF-α and IL-1β genes were analyzed by RTD-PCR. The basal (prestimuli) expression of TLR2, TLR3, and TLR4 (*A*) and TNF-α and IL-1β (*B*) did not differ significantly between the two groups. The TLR ligand–induced expression of TNF-α (*C*) and IL-1β (*D*) was downregulated in the monocytes of patients with diabetes. Data are expressed as means ± SEM. *$P < 0.05$, **$P < 0.01$.**

tosed *E. coli* and A1C levels among the patients (data not shown).

Next, we assessed the responsiveness of monocytes to external pathogenic stimuli in vitro. Monocytes typically express pattern-recognition molecules such as the TLRs that are important for innate immunity against various pathogens (13,14). The expression levels of TLR2, TLR3, and TLR4 were not significantly different between monocytes from patients with diabetes and those from healthy volunteers, as assessed by RTD-PCR (Fig. 3*A*) and flow cytometry (data not shown). We also found that transcriptional expression of TLR signal molecules (MyD88, IRAK1, and TRAF6 for TLR2 and TLR4 signaling and TRIF for TLR3 signaling) was not altered in diabetic monocytes compared with nondiabetic monocytes (data not shown). Next, we exposed the monocytes from the patients with diabetes and healthy volunteers to the TLR ligands, PGN (a TLR2 ligand), Poly (I:C) (a TLR3 ligand), and LPS (a TLR4 ligand) and measured the expression of the proinflammatory cytokine genes, TNF-α and IL-1β. After incubation, the expression of the cytokines was not significantly different between the groups (Fig. 3*B*), but the responsiveness to PGN, Poly (I:C), and LPS was significantly attenuated in monocytes from patients with diabetes compared with those from healthy volunteers as assessed by RTD-PCR (Fig. 3*C* and *D*). These results demonstrate that the monocytes of patients with diabetes are functionally impaired, which implies that they could contribute to immune deficiency in diabetes.

ER stress is a molecular feature of impaired monocytes. To elucidate the molecular features of the diabetic monocytes that were distinctly susceptible to apoptosis, DNA microarray analysis was performed on CD14$^+$ cells isolated from five randomly selected patients with diabetes and five healthy volunteers. These subjects demonstrated clinical features near the median of all study subjects. Unsupervised hierarchic clustering analysis was performed to assess the gene expression profiles of monocytes obtained from patients with diabetes and healthy volunteers; 17,184 filtered genes were evaluated after excluding genes that were not expressed or those with low expression levels that prevented their analysis in 50% of the cases. As shown in Fig. 4*A*, two completely discernible clusters formed between the patients with diabetes and the healthy volunteers.

We identified 813 genes that were upregulated in the monocytes from patients with diabetes compared with those of healthy volunteers ($P < 0.05$, Student *t* test). Analysis of the biological processes concerning these genes was performed using GenMAPP. The identified genes were shown to be involved in posttranslational protein modification systems occurring in the Golgi apparatus or were involved in ER stress (Table 2 and supplementary Table 1, available in an online appendix at http://diabetes.diabetesjournals.org/cgi/content/full/db09-0659/DC1). The elevated expression of genes related to ER stress, such as CHOP and BiP, was confirmed using RTD-PCR; the expression of these genes was significantly higher in the monocytes from the 33

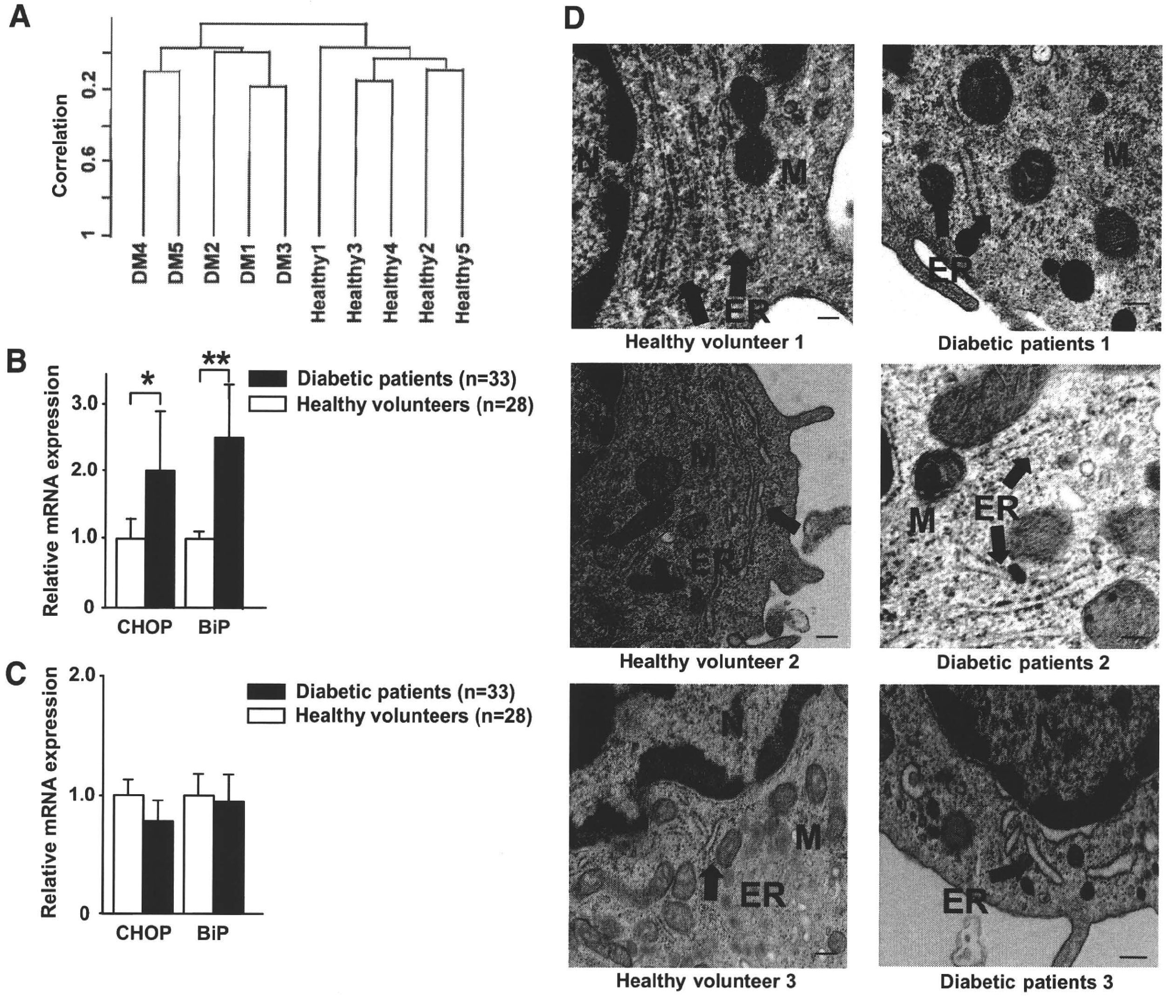

FIG. 4. Monocytes of patients with diabetes were under ER stress. *A*: The gene expression profiles of representative vulnerable CD14$^+$ monocytes obtained from five patients with diabetes and five healthy volunteers were analyzed using a DNA microarray. Unsupervised hierarchic clustering using 17,184 filtered genes produced two clusters that separated the patients with diabetes from the healthy volunteers without exception. *B* and *C*: The gene expression levels of the ER stress markers, such as CHOP and BiP, on CD14$^+$ monocytes and CD4$^+$ T-cells obtained from 33 patients with diabetes and 28 healthy volunteers were analyzed using RTD-PCR. *B*: The expression levels of CHOP and BiP in monocytes of patients with diabetes were significantly upregulated, compared with the monocytes of healthy volunteers. Data are expressed as means ± SEM. *$P < 0.05$, **$P < 0.01$. *C*: The expression levels of CHOP and BiP in T-cells of patients with diabetes were similar to those of healthy volunteers. Data are expressed as means ± SEM. *D*: Monocytes were obtained from three healthy volunteers and three patients with diabetes (healthy volunteer 1: 64-year-old man, A1C 5.7%; healthy volunteer 2: 66-year-old man, A1C 4.9%; healthy volunteer 3: 68-year-old woman, A1C 5.6%; diabetic patient 1: 56-year-old man, A1C 9.1%; diabetic patient 2: 64-year-old woman, A1C 8.2%; diabetic patient 3: 71-year-old man, A1C 10.2%) and examined using electron microscopy. In the three patients with diabetes, the concentric, continuous, and regular layer structures of the ER were corrupted, with fewer ribosomes on the ER membrane compared with the ER of the healthy volunteer. ER, endoplasmic reticulum; M, mitochondrion; N, nucleus. Scale bars indicate 100 nm.

patients with diabetes than in those from the 28 healthy volunteers (Fig. 4*B*). In contrast, no significant difference in the expression of these genes was observed in CD4$^+$ T-cells from patients with diabetes and healthy volunteers (Fig. 4*C*).

Electron microscopy further confirmed ER stress in the monocytes derived from patients with diabetes. As shown in Fig. 4*D*, morphologic alterations of the ER such as corruption of concentric, continuous, and regular layer structure and a decreased number of ribosomes on the ER membrane were evident from the electron photomicrographic images.

ER stress–induced apoptosis and attenuation of TLR signaling in human monocytes. The results described above indicated that the monocytes from patients with diabetes have compromised immunologic function and that ER stress is a distinct feature in these cells. To determine whether ER stress could be a mechanism underlying the observed increase in apoptosis and decreased responsiveness to TLR ligands, CD14$^+$ cells isolated from a healthy volunteer were treated with the ER stress inducer, tunicamycin (1 μg/ml), in AIM-V media. As shown in Fig. 5*A* and *B*, an increased number of apoptotic cells was observed among monocytes treated with tunica-

TABLE 2
Biological processes for upregulated genes in monocytes of diabetic patients

	Z score	Permute *P* value
MAPP name		
Golgi apparatus	3.383	0.000
Ribosomal proteins	3.691	0.002
Unfold protein binding	2.471	0.026
Intracellular protein transport	2.310	0.029
Enzyme-linked receptor protein signaling pathway	2.175	0.042
Nuclear receptor	2.316	0.043
Gametogenesis	−1.998	0.049

mycin compared with untreated monocytes after >6 h of incubation. Treatment of monocytes with a higher concentration of tunicamycin (5 μg/ml) induced more apoptosis (Fig. 5*A* and *B*), and when monocytes were treated with tunicamycin for 12 h, the activity of the proapoptotic protease, caspase-3, significantly increased (Fig. 5*C*). Treatment with tunicamycin coordinately decreased the expression of BCL-2 (Fig. 5*D*) and increased the expression of the ER stress markers, CHOP and BiP (Fig. 5*E*). These results suggest that ER stress promotes apoptosis of human monocytes.

Next, we investigated how tunicamycin-induced ER stress affected the responsiveness of human monocytes to TLR ligands. Treatment of monocytes with tunicamycin for 6 h did not affect the transcriptional and translational expression of TLR2 and TLR4 (data not shown). As shown in Fig. 6*A–C*, however, the expression of the proinflammatory cytokines TNF-α, IL-1β, and IL-6 was downregulated after stimulation with TLR2 and TLR4 ligands. Furthermore, the production of TNF-α, IL-1β, and IL-6 in media was measured by ELISA and found to decrease after treatment of human monocytes with tunicamycin and after stimulation with TLR2 or TLR4 ligands (Fig. 6*D–F*). However, tunicamycin-induced ER stress did not affect expression after treatment of monocytes with the TLR3 ligand, Poly (I:C) (data not shown).

DISCUSSION

In the present study, we observed that PBMCs from patients with diabetes were more susceptible to apoptosis compared with PBMCs from healthy volunteers and that

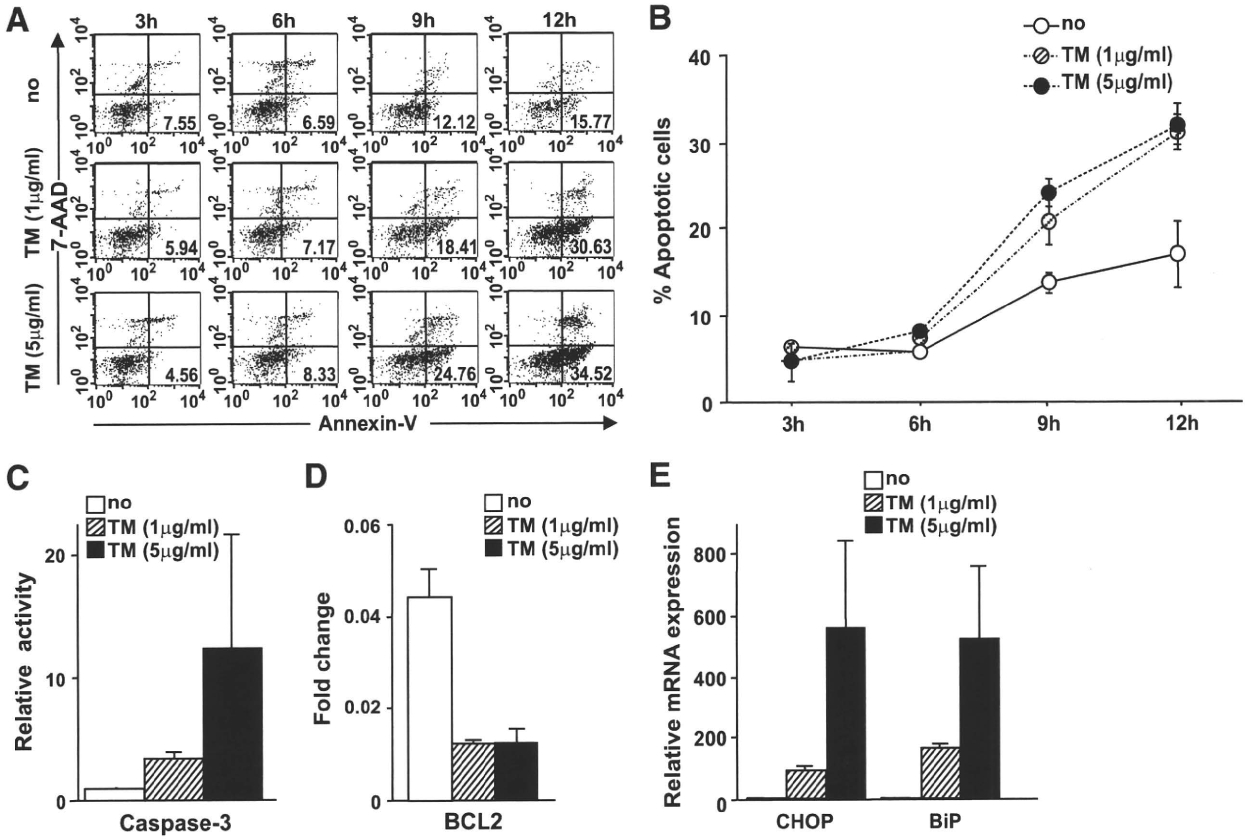

FIG. 5. ER stress enhanced the susceptibility of human monocytes to apoptosis. *A* and *B*: Human CD14⁺ monocytes obtained from a healthy volunteer were incubated in AIM-V culture media supplemented with tunicamycin (TM) (1 or 5 μg/ml). The frequency of apoptotic cells was analyzed by flow cytometry every 3 h for 12 h. More apoptotic cells were observed among monocytes treated with tunicamycin for >6 h of incubation, compared with untreated monocytes. *A*: Representative scattergram of annexin-V and 7-AAD for monocytes treated with tunicamycin. The numbers in each quadrant indicate the percentage of apoptotic cells. *B*: Apoptotic cells were assessed in triplicate for each condition. Data are expressed as means ± SEM. *C*: Caspase-3 activity in monocytes treated with tunicamycin increased significantly at 12 h of incubation. *D*: The BCL-2 expression in monocytes incubated with tunicamycin for 12 h was downregulated. *E*: The expression levels of the ER stress markers CHOP and BiP in monocytes incubated with tunicamycin for 12 h were significantly upregulated. Data are expressed as means ± SEM of three independent experiments. □, No treatment; ▨, treatment with tunicamycin (1 μg/ml); ■, treatment with tunicamycin (5 μg/ml).

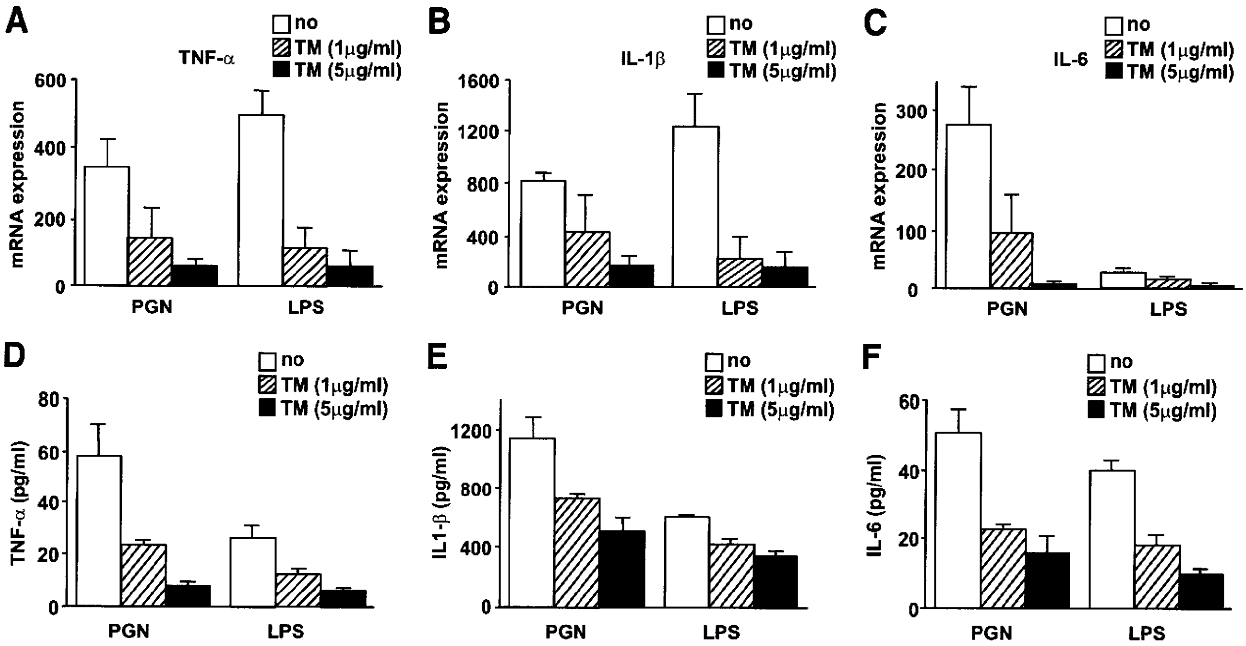

FIG. 6. Expression of proinflammatory cytokines in response to TLR ligand stimuli decreased in human monocytes treated with tunicamycin (TM). Isolated human CD14$^+$ monocytes were incubated in AIM-V culture media with tunicamycin (1 or 5 μg/ml) and stimulated using TLR ligands, PGN, and LPS for 6 h. *A–C*: RTD-PCR analysis showed that the expression of TNF-α (*A*), IL-1β (*B*), and IL-6 (*C*) was downregulated in human CD14$^+$ monocytes treated with tunicamycin, especially at the higher concentration (5 μg/ml). *D–F*: ELISA showed that the production of TNF-α (*D*), IL-1β (*E*), and IL-6 (*F*) in culture media decreased in human monocytes treated with tunicamycin, especially at the higher concentration (5 μg/ml). Data are expressed as means ± SEM of four independent experiments. □, No treatment; ▨, treatment with tunicamycin (1 μg/ml); ■, treatment with tunicamycin (5 μg/ml).

CD14$^+$ monocytes comprised the primary PBMC subpopulation undergoing apoptosis. We also found that CD14$^+$ monocytes from patients with diabetes were hyporesponsive to TLR ligands and that they had attenuated phagocytotic activity. Transcriptional analysis and electron microscopy revealed the presence of ER stress in the affected diabetic monocytes. Consistently, monocytes isolated from nondiabetic patients showed a similar increase in apoptosis and a weakened response to TLR ligands, when they were treated with tunicamycin, indicating that ER stress may be a pivotal mechanism underlying the decreased immunologic function observed in patients with diabetes.

As innate immune-defense mediators, monocytes are capable of ingesting exogenous pathogens to protect the host from infectious diseases. Previous studies have shown that phagocytosis in diabetic neutrophils and monocytes is attenuated (10,11). Similarly, in our study population, monocytes from patients with diabetes were less capable of phagocytosing *E. coli* pathogens compared with monocytes derived from healthy volunteers. This novel finding might explain, at least in part, the decrease in immune function characteristic of patients with diabetes (16). Nevertheless, the detailed mechanisms underlying diabetes-induced decreases in phagocytotic activity remain unclear, because simple high-glucose concentration neither affected the phagocytotic activity and TLR expression nor induced ER stress in nondiabetic monocytes in vitro (data not shown).

The TLRs are pattern-recognition receptors that are important for recognizing pathogens, inducing proinflammatory responses, and preventing the host from acquiring infectious diseases (17–20). The expression of TLR2, TLR3, and TLR4 in CD14$^+$ monocytes was similar between patients with diabetes and healthy volunteers. The administration of a high dose of insulin downregulates TLR expression (21). Transformed monocyte-lineage blastoma cells showed increased TLR expression under hyperglycemic conditions in vitro (22). Type 2 diabetes is characterized as a state of inadequately controlled glycemia associated with hyperinsulinemia due to peripheral insulin resistance (1). Taken together, the TLR expression may be affected by hyperglycemia and hyperinsulinemia in a complex manner. In contrast to the previous finding that monocytes from patients with diabetes were hypersensitive to the TLR ligand, LPS (23,24), we observed that the TNF-α and IL-1β expression from monocytes derived from patients with type 2 diabetes diminished after exposure to PGN, Poly I:C, and LPS—ligands of the TLR2, TLR3, and TLR4 receptors, respectively. These data suggest that diabetes perturbs signaling downstream of the TLRs. In this study, we collected CD14$^+$ monocytes from PBMCs via enrichment using magnetic beads; this protocol was used to remove T-cells, NK cells, B-cells, dendritic cells, and basophils from the PBMC mixture. This is in contrast to the methodology used to isolate these cells in many other studies, in which monocytes were obtained as adherent cells in the culture dish or by a rosetting technique (25,26). CD14$^+$ cells have been shown to be composed of multiple subtypes of activated states; the classical monocyte-isolation methods used in the other studies might unknowingly remove the fraction of monocytes that are susceptible to apoptosis (27). More than half of the CD14$^+$ diabetic monocytes isolated in this study were dead after 12-h incubation, even in media containing physiological concentration of glucose (data not shown).

Our current data showing attenuation of TLR responsiveness to ligands in diabetic monocytes suggest that initial immune responses that are normally triggered by viruses, bacteria, and parasites could be impaired in diabetes, which is consistent with epidemiologic data showing a high incidence of infection in patients with diabetes (3–5).

Gene expression and electron microscopic analysis of monocytes derived from patients with diabetes showed active signatures of ER stress; this is important because ER is an organelle essential for the proper folding and glycosylation of proteins after protein synthesis (28). When cells are under ER stress, protein kinase R–like ER kinase, inositol-requiring enzyme 1, and activating transcription factor 6 are activated and function in the adaptation to stress, proper folding of proteins, and removal of harmful unfolded proteins, respectively (29,30). However, prolonged ER stress leads to apoptotic cell death, which is mediated by CHOP (31). CHOP is a crucial and specific molecule for ER stress–induced apoptosis and alters the transcription of the *BCL-2* gene family members (32). The current study showed that diabetic monocytes had increased levels of ER stress–related apoptotic molecules. Moreover, nondiabetic monocytes treated with tunicamycin, an ER stress inducer, underwent apoptosis in a manner similar to monocytes derived from patients with diabetes. From these data, we conclude that ER stress contributes to the susceptibility of diabetic monocytes to apoptosis.

We also observed that tunicamycin-induced ER stress diminished TLR2 and TLR4 signaling without altering expression of TLRs. Tunicamycin induces ER stress by disturbing N-linked glycosylation (33), and previous reports suggest that perturbations in this glycosylation attenuate TLR2 and TLR4 signaling in vitro (34,35). Hence, these data collectively indicate that ER stress may underlie decreases in TLR2 and TLR4 signaling and affect immune function in patients with diabetes.

TLR3 signaling is different from the other TLR signaling pathway; for example, it is independent of MyD88. TLR2 and TLR4 are expressed on the cell surface, whereas TLR3 is expressed in intracellular compartments such as endosomes (13), and its ligands require internalization before signaling occurs. This suggests that disturbances in TLR3 signaling in diabetic monocytes may be due to reasons other than ER stress. Further investigations are needed to elucidate the detailed mechanisms of attenuated TLR signaling in monocytes from patients with diabetes.

ER stress has been shown to be a mainstay of the diabetic condition. Its pathologic importance in diabetes is especially important in pancreatic β-cells, in which glucose toxicity results in ER stress and insufficient insulin secretion (36–38). The current study suggests that monocytes are yet another population of cells vulnerable to hyperglycemia-induced ER stress and dysfunction. Nevertheless, the mechanisms that render pancreatic β-cells and monocytes vulnerable to ER stress in patients with diabetes remain uncertain.

Diabetes is considered a chronic inflammatory disease. Activated macrophages that produce proinflammatory cytokines such as TNF-α, IL-1β, and IL-6 are thought to contribute to insulin resistance in muscle and adipose tissues (39,40). Furthermore, the atherosclerotic complications in patients with diabetes have a basis in inflammation; local inflammatory foci in atherosclerotic lesions are commonly composed of foam cells derived from activated macrophages (41,42). Further studies are needed to determine whether different subpopulations of monocyte-derived cells, for example, systemically circulating and locally residing inflammatory cells, are susceptible to hyperglycemia-induced ER stress and dysfunction.

In conclusion, our findings show that $CD14^+$ monocytes are susceptible to ER stress–induced alterations in inflammatory signaling and apoptosis, which may play a role in the decreased immune function observed in patients with diabetes. Further investigations are needed to discern the mechanisms of diabetes-induced ER stress and perturbations in inflammatory signaling in $CD14^+$ monocytes.

ACKNOWLEDGMENTS

No potential conflicts of interest relevant to this article were reported.

We thank Dr. Iseki for valuable advice and critical comments on electron microscopic examination about ER of monocytes.

REFERENCES

1. Stumvoll M, Goldstein BJ, van Haeften TW. Type 2 diabetes: principles of pathogenesis and therapy. Lancet 2005;365:1333–1346
2. Zimmet P, Alberti KG, Shaw J. Global and societal implications of the diabetes epidemic. Nature 2001;414:782–787
3. Joshi N, Caputo GM, Weitekamp MR, Karchmer AW. Infections in patients with diabetes mellitus. N Engl J Med 1999;341:1906–1912
4. Shah BR, Hux JE. Quantifying the risk of infectious diseases for people with diabetes. Diabetes Care 2003;26:510–513
5. Finney SJ, Zekveld C, Elia A, Evans TW. Glucose control and mortality in critically ill patients. JAMA 2003;290:2041–2047
6. Dunn GP, Old LJ, Schreiber RD. The immunobiology of cancer immunosurveillance and immunoediting. Immunity 2004;21:137–148
7. Karin M, Lawrence T, Nizet V. Innate immunity gone awry: linking microbial infections to chronic inflammation and cancer. Cell 2006;124:823–835
8. Delamaire M, Maugendre D, Moreno M, Le Goff MC, Allannic H, Genetet B. Impaired leucocyte functions in diabetic patients. Diabet Med 1997;14:29–34
9. Geerlings SE, Hoepelman AI. Immune dysfunction in patients with diabetes mellitus (DM). FEMS Immunol Med Microbiol 1999;26:259–265
10. Katz S, Klein B, Elian I, Fishman P, Djaldetti M. Phagocytotic activity of monocytes from diabetic patients. Diabetes Care 1983;6:479–482
11. Geisler C, Almdal T, Bennedsen J, Rhodes JM, Kølendorf K. Monocyte functions in diabetes mellitus. Acta Pathol Microbiol Immunol Scand C 1982;90:33–37
12. Takamura T, Honda M, Sakai Y, Ando H, Shimizu A, Ota T, Sakurai M, Misu H, Kurita S, Matsuzawa-Nagata N, Uchikata M, Nakamura S, Matoba R, Tanino M, Matsubara K, Kaneko S. Gene expression profiles in peripheral blood mononuclear cells reflect the pathophysiology of type 2 diabetes. Biochem Biophys Res Commun 2007;361:379–384
13. Akira S, Uematsu S, Takeuchi O. Pathogen recognition and innate immunity. Cell 2006;124:783–801
14. Pasare C, Medzhitov R. Toll-like receptors: linking innate and adaptive immunity. Microbes Infect 2004;6:1382–1387
15. Tateno M, Honda M, Kawamura T, Honda H, Kaneko S. Expression profiling of peripheral-blood mononuclear cells from patients with chronic hepatitis C undergoing interferon therapy. J Infect Dis 2007;195:255–267
16. Stuart LM, Ezekowitz RA. Phagocytosis and comparative innate immunity: learning on the fly. Nat Rev Immunol 2008;8:131–141
17. Thoma-Uszynski S, Stenger S, Takeuchi O, Ochoa MT, Engele M, Sieling PA, Barnes PF, Rollinghoff M, Bolcskei PL, Wagner M, Akira S, Norgard MV, Belisle JT, Godowski PJ, Bloom BR, Modlin RL. Induction of direct antimicrobial activity through mammalian toll-like receptors. Science 2001;291:1544–1547
18. Barton GM, Medzhitov R. Toll-like receptor signaling pathways. Science 2003;300:1524–1525
19. Sabroe I, Parker LC, Dower SK, Whyte MK. The role of TLR activation in inflammation. J Pathol 2008;214:126–135
20. Iwasaki A, Medzhitov R. Toll-like receptor control of the adaptive immune responses. Nat Immunol 2004;10:987–995
21. Ghanim H, Mohanty P, Deopurkar R, Sia CL, Korzeniewski K, Abuaysheh S, Chaudhuri A, Dandona P. Acute modulation of Toll-like receptors by insulin. Diabetes Care 2008;31:1827–1831

22. Dasu MR, Devaraj S, Zhao L, Hwang DH, Jialal I. High glucose induces toll-like receptor expression in human monocytes: mechanism of activation. Diabetes 2008;57:3090–3098
23. Desfaits AC, Serri O, Renier G. Normalization of plasma lipid peroxides, monocyte adhesion, and tumor necrosis factor-alpha production in NIDDM patients after gliclazide treatment. Diabetes Care 1998;21:487–493
24. Ohno Y, Aoki N, Nishimura A. In vitro production of interleukin-1, interleukin-6, and tumor necrosis factor-alpha in insulin-dependent diabetes mellitus. J Clin Endocrinol Metab 1993;77:1072–1077
25. Renier G, Mamputu JC, Serri O. Benefits of gliclazide in the atherosclerotic process: decrease in monocyte adhesion to endothelial cells. Metabolism 2003;52:13–18
26. Serbina NV, Jia T, Hohl TM, Pamer EG. Monocyte-mediated defense against microbial pathogens. Annu Rev Immunol 2008;26:421–452
27. Wahl LM, Wahl SM, Smythies LE, Smith PD. Isolation of human monocyte populations. Curr Protoc Immunol 2006;Chapter 7:Unit 7.6A
28. Ron D, Walter P. Signal integration in the endoplasmic reticulum unfolded protein response. Nat Rev Mol Cell Biol 2007;8:519–529
29. Xu C, Bailly-Maitre B, Reed JC. Endoplasmic reticulum stress: cell life and death decisions. J Clin Invest 2005;115:2656–2664
30. Bukau B, Weissman J, Horwich A. Molecular chaperones and protein quality control. Cell 2006;125:443–451
31. Wang XZ, Ron D. Stress-induced phosphorylation and activation of the transcription factor CHOP (GADD153) by p38 MAP Kinase. Science 1996;272:1347–1349
32. McCullough KD, Martindale JL, Klotz LO, Aw TY, Holbrook NJ. Gadd153 sensitizes cells to endoplasmic reticulum stress by down-regulating Bcl2 and perturbing the cellular redox state. Mol Cell Biol 2001;21:1249–1259
33. Kataoka H, Yasuda M, Iyori M, Kiura K, Narita M, Nakata T, Shibata K. Roles of N-linked glycans in the recognition of microbial lipopeptides and lipoproteins by TLR2. Cell Microbiol 2006;8:1199–1209
34. Ohnishi T, Muroi M, Tanamoto K. N-linked glycosylations at Asn(26) and Asn(114) of human MD-2 are required for toll-like receptor 4-mediated activation of NF-kappaB by lipopolysaccaharide. J Immunol 2001;167: 3354–3359
35. Weber AN, Morse MA, Gay NJ. Four N-linked glycosylation sites in human toll-like receptor 2 cooperate to direct efficient biosynthesis and secretion. J Biol Chem 2004;279:34589–34594
36. Ozcan U, Cao Q, Yilmaz E, Lee AH, Iwakoshi NN, Ozdelen E, Tuncman G, Görgün C, Glimcher LH, Hotamisligil GS. Endoplasmic reticulum stress links obesity, insulin action, and type 2 diabetes. Science 2004;306:457–461
37. Oyadomari S, Takeda K, Takiguchi M, Gotoh T, Matsumoto M, Wada I, Akira S, Araki E, Mori M. Nitric oxide-induced apoptosis in pancreatic beta cells is mediated by the endoplasmic reticulum stress pathway. Proc Natl Acad Sci U S A 2001;98:10845–10850
38. Schenk S, Saberi M, Olefsky JM. Insulin sensitivity: modulation by nutrients and inflammation. J Clin Invest 2008;118:2992–3002
39. Kahn SE, Hull RL, Utzschneider KM. Mechanisms linking obesity to insulin resistance and type 2 diabetes. Nature 2006;444:840–846
40. Wellen KE, Hotamisligil GS. Inflammation, stress, and diabetes. J Clin Invest 2005;115:1111–1119
41. Brownlee M. Biochemistry and molecular cell biology of diabetic complications. Nature 2001;414:813–820
42. Liang CP, Han S, Senokuchi T, Tall AR. The macrophage at the crossroads of insulin resistance and atherosclerosis. Circ Res 2007;100:1546–1555

 doi:10.1111/j.1365-2249.2010.04246.x

Prolonged recurrence-free survival following OK432-stimulated dendritic cell transfer into hepatocellular carcinoma during transarterial embolization

Y. Nakamoto,* E. Mizukoshi,* M. Kitahara,* F. Arihara,* Y. Sakai,* K. Kakinoki,* Y. Fujita,* Y. Marukawa,* K. Arai,* T. Yamashita,* N. Mukaida,† K. Matsushima,‡ O. Matsui§ and S. Kaneko*

*Disease Control and Homeostasis, Graduate School of Medicine, †Division of Molecular Bioregulation, Cancer Research Institute, Kanazawa University, §Department of Radiology, Graduate School of Medicine, Kanazawa University, Kanazawa, and ‡Department of Molecular Preventive Medicine, Graduate School of Medicine, University of Tokyo, Tokyo, Japan

Accepted for publication 19 July 2010
Correspondences: S. Kaneko, Disease Control and Homeostasis, Graduate School of Medical Science, Kanazawa University, 13-1 Takara-machi, Kanazawa 920-8641, Japan.
E-mail: skaneko@m-kanazawa.jp

Summary

Despite curative locoregional treatments for hepatocellular carcinoma (HCC), tumour recurrence rates remain high. The current study was designed to assess the safety and bioactivity of infusion of dendritic cells (DCs) stimulated with OK432, a streptococcus-derived anti-cancer immunotherapeutic agent, into tumour tissues following transcatheter hepatic arterial embolization (TAE) treatment in patients with HCC. DCs were derived from peripheral blood monocytes of patients with hepatitis C virus-related cirrhosis and HCC in the presence of interleukin (IL)-4 and granulocyte-macrophage colony-stimulating factor and stimulated with 0·1 KE/ml OK432 for 2 days. Thirteen patients were administered with 5×10^6 of DCs through arterial catheter during the procedures of TAE treatment on day 7. The immunomodulatory effects and clinical responses were evaluated in comparison with a group of 22 historical controls treated with TAE but without DC transfer. OK432 stimulation of immature DCs promoted their maturation towards cells with activated phenotypes, high expression of a homing receptor, fairly well-preserved phagocytic capacity, greatly enhanced cytokine production and effective tumoricidal activity. Administration of OK432-stimulated DCs to patients was found to be feasible and safe. Kaplan–Meier analysis revealed prolonged recurrence-free survival of patients treated in this manner compared with the historical controls ($P = 0{\cdot}046$, log-rank test). The bioactivity of the transferred DCs was reflected in higher serum concentrations of the cytokines IL-9, IL-15 and tumour necrosis factor-α and the chemokines CCL4 and CCL11. Collectively, this study suggests that a DC-based, active immunotherapeutic strategy in combination with locoregional treatments exerts beneficial anti-tumour effects against liver cancer.

Keywords: dendritic cells, hepatocellular carcinoma, immunotherapy, recurrence-free survival, transcatheter hepatic arterial embolization

Introduction

Many locoregional therapeutic approaches including surgical resection, radiofrequency ablation (RFA) and transcatheter hepatic arterial embolization (TAE) have been taken in the search for curative treatments of hepatocellular carcinoma (HCC). Despite these efforts, tumour recurrence rates remain high [1,2], probably because active hepatitis and cirrhosis in the surrounding non-tumour liver tissues causes *de novo* development of HCC [3,4]. One strategy to reduce tumour recurrence is to enhance anti-tumour immune responses that may induce sufficient inhibitory effects to prevent tumour cell growth and survival [5,6]. Dendritic cells (DCs) are the most potent type of antigen-presenting cells in the human body, and are involved in the regulation of both innate and adaptive immune responses [7]. DC-based immunotherapies are believed to contribute to the eradication of residual and recurrent tumour cells.

To enhance tumour antigen presentation to T lymphocytes, DCs have been transferred with major histocompatibility complex (MHC) class I and class II genes [8] and co-stimulatory molecules, e.g. CD40, CD80 and CD86 [9,10], and loaded with tumour-associated antigens, including tumour lysates, peptides and RNA transfection [11]. To induce natural killer (NK) and natural killer T (NK T) cell activation, DCs have been stimulated and modified to

Table 1. Patient characteristics.

Patient no.	Gender	Age (years)	HLA	TNM stages	No. of tumours	Largest tumour (mm)	Child–Pugh	KPS	Post-TAE Rx
1	M	60	A11 A33	III	5	35	B	100	RFA
2	M	57	A11 A24	III	1	21	B	100	RFA
3	M	57	A11 A31	III	2	39	B	100	RFA
4	M	77	A2 A24	III	2	35	A	100	RFA
5	F	83	A11 A24	III	3	29	B	100	RFA
6	F	74	A2 A24	II	1	35	A	100	RFA
7	F	72	A24 A33	III	3	41	B	100	RFA
8	F	65	A2 A11	II	4	12	B	100	RFA
9	M	71	A2 A11	II	4	16	A	100	RFA
10	M	79	A11 A24	III	2	40	A	100	RFA
11	M	71	A2 A24	II	1	28	A	100	RFA
12	M	56	A2 A26	III	2	25	B	100	RFA
13	M	64	A2 A33	III	2	37	B	100	RFA

M, male; F, female; TNM, tumour–node–metastasis; Child–Pugh, Child–Pugh classification; KPS, Karnofsky performance scores; TAE, transcatheter arterial embolization; Rx, treatment; HCC, hepatocellular carcinoma; HLA, human leucocyte antigen; RFA, percutaneous radiofrequency ablation.

produce larger amounts of cytokines, e.g. interleukin (IL)-12, IL-18 and type I interferons (IFNs) [10,12]. Furthermore, DC migration into secondary lymphoid organs could be induced by expression of chemokine genes, e.g. C-C chemokine receptor-7 (CCR7) [13], and by maturation using inflammatory cytokines [14], matrix metalloproteinases and Toll-like receptor (TLR) ligands [15].

DCs stimulated with OK432, a penicillin-inactivated and lyophilized preparation of *Streptococcus pyrogenes*, were suggested recently to produce large amounts of T helper type 1 (Th1) cytokines, including IL-12 and IFN-γ and enhance cytotoxic T lymphocyte activity compared to a standard mixture of cytokines [tumour necrosis factor-α (TNF-α), IL-1β, IL-6 and prostaglandin E_2 (PGE_2)] [16]. Furthermore, because OK432 modulates DC maturation through TLR-4 and the β_2 integrin system [16,17] and TLR-4-stimulated DCs can abrogate the activity of regulatory T cells [18], OK432-stimulated DCs may contribute to the induction of anti-tumour immune responses partly by reducing the activity of suppressor cells. Recently, in addition to the orchestration of immune responses, OK432-activated DCs have themselves been shown to mediate strong, specific cytotoxicity towards tumour cells via CD40/CD40 ligand interactions [19].

We have reported recently that combination therapy using TAE together with immature DC infusion is safe for patients with cirrhosis and HCC [20]. DCs were infused precisely into tumour tissues and contributed to the recruitment and activation of immune cells *in situ*. However, this approach by itself yielded limited anti-tumour effects due probably to insufficient stimulation of immature DCs (the preparation of which seems closely related to therapeutic outcome [21,22]). The current study was designed to assess the safety and bioactivity of OK432-stimulated DC infusion into tumour tissues following TAE treatment in patients with cirrhosis and HCC. In addition to documenting the safety of this approach, we found that patients treated with OK432-stimulated DCs displayed unique cytokine and chemokine profiles and, most importantly, experienced prolonged recurrence-free survival.

Patients and methods

Patients

Inclusion criteria were a radiological diagnosis of primary HCC by computed tomography (CT) angiography, hepatitis C virus (HCV)-related HCC, a Karnofsky score of ≥ 70%, an age of ≥ 20 years, informed consent and the following normal baseline haematological parameters (within 1 week before DC administration): haemoglobin ≥ 8·5 g/dl; white cell count ≥ 2000/μl; platelet count ≥ 50 000/μl; creatinine < 1·5 mg/dl and liver damage A or B [23].

Exclusion criteria included severe cardiac, renal, pulmonary, haematological or other systemic disease associated with a discontinuation risk; human immunodeficiency virus (HIV) infection; prior history of other malignancies; history of surgery, chemotherapy or radiation therapy within 4 weeks; immunological disorders including splenectomy and radiation to the spleen; corticosteroid or anti-histamine therapy; current lactation; pregnancy; history of organ transplantation; or difficulty in follow-up.

Thirteen patients (four women and nine men) presenting at Kanazawa University Hospital between March 2004 and June 2006 were enrolled into the study, with an age range from 56 to 83 years (Table 1). Patients with verified radiological diagnoses of HCC stage II or more were eligible and enrolled in this study. In addition, a group of 22 historical controls (nine women and 13 men) treated with TAE without DC administration between July 2000 and September 2007 was included in this study. All patients received RFA therapy to increase the locoregional effects 1 week later [24].